UNIVERSIDADE FEDERAL DE VIÇOSA

EDUARDO JOSÉ HAVERROTH

THE ROLE OF ABSCISIC ACID AND SECONDARY GROWTH ON EMBOLISM RESISTANCE AND DROUGHT TOLERANCE IN HERBACEOUS PLANTS

VIÇOSA - MINAS GERAIS
2023

EDUARDO JOSÉ HAVERROTH

THE ROLE OF ABSCISIC ACID AND SECONDARY GROWTH ON EMBOLISM RESISTANCE AND DROUGHT TOLERANCE IN HERBACEOUS PLANTS

Thesis submitted to the Plant Physiology Graduate Program of the Universidade Federal de Viçosa in partial fulfillment of the requirements for the degree of *Doctor Scientiae*.

Adviser: Samuel Cordeiro Vitor Martins

Co-advisers: Amanda Ávila Cardoso
Agustin Zsögön
Fábio Murilo DaMatta

VIÇOSA - MINAS GERAIS
2023

Ficha catalográfica elaborada pela Biblioteca Central da Universidade Federal de Viçosa - Campus Viçosa

T

H387p
2023

Haverroth, Eduardo José, 1994-
The role of abscisic acid and secondary growth on embolism resistance and drought tolerance in herbaceous plants / Eduardo José Haverroth. - Viçosa, MG, 2023.
1 tese eletrônica (81 f.): il. (algumas color.).

Texto em inglês
.

Orientador: Samuel Cordeiro Vitor Martins.
Tese (doutorado) - Universidade Federal de Viçosa, Departamento de Biologia Vegetal, 2023.
Inclui bibliografia.
DOI: https://doi.org/10.47328/ufvbbt.2023.464
Modo de acesso: World Wide Web.

1. Fisiologia vegetal. 2. Plantas - Relações hídricas. 3. Plantas - Resistência à seca. 4. Plantas - Crescimento. 5. Cavitação. I. Martins, Samuel Cordeiro Vitor, 1986-. II. Universidade Federal de Viçosa. Departamento de Biologia Vegetal. Programa de Pós-Graduação em Fisiologia Vegetal. III. Título.

CDD 22. ed. 571.2

Bibliotecário(a) responsável: Bruna Silva CRB-6/2552

EDUARDO JOSÉ HAVERROTH

THE ROLE OF ABSCISIC ACID AND SECONDARY GROWTH ON EMBOLISM RESISTANCE AND DROUGHT TOLERANCE IN HERBACEOUS PLANTS

Thesis submitted to the Plant Physiology Graduate Program of the Universidade Federal de Viçosa in partial fulfillment of the requirements for the degree of *Doctor Scientiae*.

APPROVED: July 27, 2023.

Assent:

gov.br
Documento assinado digitalmente
EDUARDO JOSE HAVERROTH
Data: 01/08/2023 17:50:03-0300
Verifique em https://validar.iti.gov.br

Eduardo José Haverroth
Author

gov.br
Documento assinado digitalmente
SAMUEL CORDEIRO VITOR MARTINS
Data: 01/08/2023 22:16:23-0300
Verifique em https://validar.iti.gov.br

Samuel Cordeiro Vitor Martins
Adviser

ACKNOWLEDGEMENTS

I am thankful to the Brazilian people who pay taxes that support public, free, and high-quality education. Even though most people do not realize it, they are funding the study of youth people projecting a better and fairer future for their home country.

My deepest gratitude to my parents who have been watching and encouraging me to dream big and aim for the more ambitious steps. Thank you for understanding the absence on some important family dates. Thank you for teaching me that the right path is not always the easiest one, but with patience, talk, and effort, everything can be achieved.

To my adviser, Samuel Martins, who showed very receptiveness since the first time we met at Universidade Federal do Rio Grande do Sul, showing me the university campus around. His kindness and weightless way of dealing with work and students taught me a lot and helped me to guide my decisions during my academic journey.

To my co-adviser, Amanda Cardoso, whose enthusiasm, and hard work helped me to thrive on my thesis. Her spontaneity in planning my thesis project with me during a ludic time at a laboratory cookout, drinking beer and having good food, conquered me. Thank you for believing in me and giving me the opportunity of having an international experience in your laboratory. The challenge of helping you to start your journey in the pack certainly is my great professional achievement, which will help me to develop my “resistance” in my “secondary growth” called industry.

To the family that I built during my time in Viçosa. Kleiton for always being ready to hang out, have a beer, tell bad jokes, and listen to my complaints. Lucas for always being spontaneous and making everyone laugh at his way of choosing words. Carlos for showing that everybody needs something to get support from. Diego for showing that any time is time to hang out and get pumped. Raissa for being the most kind, lovely, and patient person, always taking care of me. Leticia for teaching me that a good friend is part of the family. Leandro for showing love by cooking delicious meals and introducing me to lovely friends.

To my friends in the United States, Rafaella, Ana Paula, Day, Amauri, Chris, and Shawn who alleviate homesickness. Having you around was indispensable to keeping my mental sanity.

To my laboratory colleagues, Leonardo, Moab, Talitha, and Matt who never measured efforts to help me during experiment times. Thank you for working as a team and making my life easier.

To the Universidade Federal de Viçosa (UFV), for the opportunity to complete the postgraduate course. To the funding institutions. To North Carolina State University (NCSU) for the opportunity of being a visiting scholar in the pack. To the phytotron staff to grow part of the plants used in my experiments. To the Coordenação de Aperfeiçoamento de Pessoal de Nível Superior (CAPES), to granting the scholarship. To the assistanship provided by the USDA Hatch project 7003279 via Cardoso Lab at NCSU.

ABSTRACT

HAVERROTH, Eduardo José, D.Sc., Universidade Federal de Viçosa, July, 2023. **The role of abscisic acid and secondary growth on embolism resistance and drought tolerance in herbaceous plants**. Adviser: Samuel Cordeiro Vitor Martins. Co-advisers: Amanda Ávila Cardoso, Agustin Zsögön and Fábio Murilo DaMatta.

Drought resistance is crucial for plant productivity in water-limited conditions. While the role of abscisic acid (ABA) in stomatal regulation is well-studied, its influence on hydraulic function beyond stomata remains understudied. Moreover, the impacts of secondary growth on xylem resistance are still poorly understood. In the first chapter, we aimed to elucidate the impact of ABA on drought-induced dysfunction by examining genotypes with divergent ABA accumulation abilities. All genotypes exhibited similar resistance to leaf and stem embolism and similar leaf hydraulic resistance. However, pronounced differences between extreme genotypes, *sitiens* (*sit*; a strong ABA-deficient mutant) and *sp12* (a transgenic line with constitutive ABA over-accumulation) were observed. The water potential inducing 50% embolism was 0.25 MPa lower in *sp12* compared to *sit*. Notably, plants with higher ABA levels (wild type and sp12) demonstrated significantly lower maximum stomatal conductance and minimum leaf conductance than ABA-deficient mutants. These variations in gas exchange were associated with ABA levels, stomatal density, and size. The elevated ABA content in plants resulted in decreased water loss, consequently leading to a delayed onset of lethal water potentials associated with embolism during drought stress. Therefore, the primary mechanism by which ABA enhances drought tolerance is through the regulation of water loss, thereby postponing the onset of dehydration and hydraulic dysfunction. In the second chapter, we focused on exploring the embolism resistance in the leaves, basal stems, and upper stems of two herbaceous species, *Solanum lycopersicum* and *Senecio minimus*, which undergo secondary growth in their mature stems. Our findings unveiled that the basal stem region with advanced secondary growth exhibited increased embolism resistance, leading to vulnerability segmentation between the basal stem and the remaining vegetative shoot. Alongside enhanced woodiness, embolism resistance in basal stems coincided with changes in anatomy and lignin content. Decreases in the pith-to-xylem area, increases in the proportion of secondary xylem conduits, and higher lignin content were observed in the basal stems. This study highlights the role of ABA in regulating drought tolerance by reducing water

loss and delaying hydraulic dysfunction. Additionally, it elucidates how secondary growth in herbaceous plants contributes to increased embolism resistance and ensures survival during drought periods while supporting the upper canopy.

Keywords: Embolism. Cavitation. ABA. *Solanum lycopersicum*. *Senecio minimus*. Stomata. Xylem. Water deficit. Secondary growth. Lignin.

RESUMO

HAVERROTH, Eduardo José, D.Sc., Universidade Federal de Viçosa, julho de 2023. **O papel do ácido abscísico e crescimento secundário na resistência ao embolismo e tolerância à seca em plantas herbáceas.** Orientador: Samuel Cordeiro Vitor Martins. Coorientadores: Amanda Ávila Cardoso, Agustin Zsögön e Fábio Murilo DaMatta.

A resistência à seca é crucial para a produtividade das plantas em condições de déficit hídrico. Embora o papel do ácido abscísico (ABA) na regulação estomática seja bem estudado, sua influência na função hidráulica além dos estômatos ainda é pouco conhecida. Além disso, os impactos do crescimento secundário em plantas herbáceas na resistência do xilema são ainda pouco compreendidos. No primeiro capítulo, objetivou-se elucidar o impacto do ABA na disfunção hidráulica induzida pela seca, examinando genótipos com diferentes capacidades de acumulação de ABA. Todos os genótipos apresentaram resistência semelhante à embolia foliar e do caule, bem como resistência hidráulica foliar semelhante. No entanto, diferenças significativas foram observadas entre os genótipos extremos, *sitiens* (*sit*; um mutante com baixa produção de ABA) e *sp12* (uma linhagem transgênica que superexpressa ABA). O potencial hídrico que induz 50% de embolia foi 0,25 MPa menor em *sp12* em comparação com *sit*. Plantas com níveis mais altos de ABA (linhagem selvagem e *sp12*) apresentaram condutância estomática máxima e condutância foliar mínima significativamente menores em comparação com mutantes deficientes em ABA. Essas variações nas trocas gasosas foram associadas aos níveis de ABA, densidade e tamanho estomático. O aumento do conteúdo de ABA nas plantas resultou em menor perda de água, o que levou ao atraso no surgimento de potenciais hídricos letais associados à embolia durante o estresse hídrico. Portanto, o principal mecanismo pelo qual o ABA melhora a tolerância à seca é através da regulação da perda de água, adiando o início da desidratação e disfunção hidráulica. No segundo capítulo, explorou-se a resistência à embolia nas folhas, base e ápice do caule de duas espécies herbáceas, *Solanum lycopersicum* e *Senecio minimus*, que passam por crescimento secundário nos caules maduros. Nossas descobertas revelaram que a região basal do caule, com crescimento secundário avançado, apresentou aumento da resistência à embolia, resultando em segmentação de vulnerabilidade entre a base do caule e o restante da parte vegetativa. A maior resistência à embolia na região basal do caule coincidiu com

alterações na anatomia e conteúdo de lignina. Observaram-se reduções na relação entre a área da medula e do xilema, aumento na proporção de condutos de xilema secundários e maior conteúdo de lignina na região basal do caule. Este estudo destaca o papel do ABA na regulação da tolerância à seca, reduzindo a perda de água da planta para a atmosfera e atrasando a disfunção hidráulica. Além disso, elucida-se como o crescimento secundário em plantas herbáceas contribui para o aumento da resistência à embolia, garantindo a sobrevivência durante períodos de seca e fornecendo suporte para o dossel superior.

Palavras-chave: Embolismo. Cavitação. ABA. *Solanum lycopersicum*. *Senecio minimus*. Estômato. Xilema. Deficit hídrico. Crescimento secundário. Lignina.

LIST OF FIGURES

CHAPTER 1

Figure 1. Stem xylem vulnerability curves obtained from the optical vulnerability technique of four tomato genotypes differing in their ability to accumulate foliar ABA: *sitiens (sit)* and *notabilis (not)* are ABA biosynthetic mutants, WT is wild type cv. Ailsa Craig, and *sp12* is a transgenic line over-accumulating ABA. Black line and shadow represent means and standard errors (*n* = 6), respectively. Green lines are replicates. Blue dashed lines represent leaf turgor loss points and red dashed lines indicate the water potentials associated with 50% of cumulative stem xylem embolism (P_{50}). The difference between these two parameters is the hydraulic safety margin (HSM). 45

Figure 2. Optical vulnerability curves obtained from leaves of four tomato genotypes differing in their ability to accumulate foliar ABA: *sitiens (sit)* and *notabilis (not)* are ABA biosynthetic mutants, WT is wild type cv. Ailsa Craig, and *sp12* is a transgenic line over-accumulating ABA. Midrib is represented by green lines, secondary veins by blue lines, and minor veins by red lines. Data are mean (highlighted lines) ± standard error (shadow) (*n* = 6). Blue dashed lines represent leaf turgor loss points and red dashed lines indicate the water potentials associated with 50% of cumulative xylem embolism for the whole leaf (P_{50}). The difference between these two parameters is the hydraulic safety margin (HSM). 46

Figure 3. Decline in leaf hydraulic conductance (K_{leaf}) during leaf dehydration for four tomato genotypes differing in their ability to accumulate foliar ABA: *sitiens (sit)* and *notabilis (not)* are ABA biosynthetic mutants, WT is wild type cv. Ailsa Craig, and *sp12* is a transgenic line over-accumulating ABA. Black continuous lines are the predicted values from the three-parameter sigmoidal equation performed using all data and shadows represent standard errors. Different symbols indicate individual plants (*n* = 6). Blue dashed lines represent leaf turgor loss points and red dashed lines indicate the water potentials associated with 50% loss in K_{leaf} (P_{50}). The difference between these two parameters is the hydraulic safety margin (HSM). 47

Figure 4. (A) Midday leaf water potential and (B) stomatal conductance (g_s) throughout a dry-down experiment of four tomato genotypes differing in their ability to accumulate foliar ABA: *sitiens (sit)* and *notabilis (not)* are ABA biosynthetic mutants, WT is wild type cv. Ailsa Craig, and *sp12* is a transgenic line over-accumulating ABA. Plants had water withheld after the first measurement and they were maintained under drought until the critical water potential of -1.30 MPa (black dashed line in A). Circles represent control plants and triangles, droughted plants. (C) Leaf hydraulic conductance (K_{leaf}) of control and droughted plants two days after irrigation was restored. (D) Plant leaf area at the end of the experiment. Data are mean ± standard error (*n* = 4). The two-way ANOVA results are shown (G=genotype; W=watering condition). Asterisks denote statistical differences (Tukey, $p<0.05$) for watering conditions (control versus drought) and letters allow comparison between treatments. See Fig S1 for representative images of plants during this experiment. 48

Figure 5. Dry-down experiment using seedlings of four tomato genotypes differing in their ability to accumulate foliar ABA: sitiens (sit) and notabilis (not) are ABA

biosynthetic mutants, WT is wild type cv. Ailsa Craig, and sp12 is a transgenic line over-accumulating ABA. (A) Whole-plant transpiration rate throughout the drought days. Black arrows indicate the day at which plants from the four genotypes wilted. (B) Total leaf area per plant. (C) Leaf hydraulic conductance (K_{leaf}) normalized by leaf area. (D) Stem hydraulic conductance (K_{stem}). (E) Root hydraulic conductance (K_{root}). Shadows and error bars represent standard error (n = 4). Letters over the error bars denote results from statistical tests (Tukey, p<0.05) conducted between genotypes. 49

Supplemental Figure S1. (A, B) Stomatal density (D_s), (C, D) guard cell length (L_s), and (E) vein density of four tomato genotypes differing in their ability to accumulate foliar ABA: *sitiens (sit)* and *notabilis (not)* are ABA biosynthetic mutants, WT is wild type cv. Ailsa Craig, and *sp12* is a transgenic line over-accumulating ABA. (F-H) Representative images of stomatal distribution (scale bar: 100 μm) from the abaxial and adaxial epidermis, and leaf venation (scale bar: 500 μm) are depicted in F, G, and H, respectively. Data are mean ± standard error (*n* = 6). Letters over the error bars denote results from statistical tests (Tukey, *p*<0.05) conducted between genotypes. 52

Supplemental Figure S2. Representative images of 60-day-old plants at the critical water potential of -1.30 MPa during the dry-down experiment and two days after irrigation was resumed (scale = 0.50 m). *Sitiens (sit)* and *notabilis (not)* are ABA biosynthetic mutants, WT is wild type cv. Ailsa Craig, and *sp12* is a transgenic line over-accumulating ABA. 53

Supplemental Figure S3. Free-hand cross-sections of stems of 60-day-old tomato plants. Sections were stained with phloroglucinol, which stains lignin in red so that the xylem area can be easily recognized. Images are from four genotypes differing in their ability to accumulate foliar ABA: *sitiens (sit)* and *notabilis (not)* are ABA biosynthetic mutants, WT is wild type cv. Ailsa Craig, and *sp12* is a transgenic line over-accumulating ABA. Scale bars: 250 μm. 54

CHAPTER 2

Figure 1. Plants of *Solanum lycopersicum* (five months old) (A) and *Senecio minimus* (seven months old) (D) and details of the upper stem (B, E) and the woody basal stem (C, F). Digital calipers (mm) are used to demonstrate differences in diameter between the upper and basal stems. Scales = 25 cm. 76

Figure 2. Optical vulnerability curves for leaf, upper and basal stem regions of *Solanum lycopersicum* and *Senecio minimus*. Solid black lines and shadows represent means ± SE (*n* = 5 for *Solanum* and *n* = 3 for *Senecio*). Red dashed lines indicate the water potential at 50% cumulative embolism (P_{50}). Color maps show the leaf water potentials at which the different embolisms occurred. 77

Figure 3. Cross sections of the upper stem and the basal stem of *Solanum lycopersicum* and *Senecio minimus* showing representative proportions of the pith and the xylem (Xy) as well as a detailed view of the primary (P Xy) and secondary xylem (S Xy). Pith-to-xylem area ratio ($P_{pith:xylem}$), proportion of secondary xylem vessel as a proportion to total xylem vessels ($P_{SecXylem}$) are shown for the herbaceous upper stem

and the woody basal stem for both species. Bars are means ± SE (*n* = 5 for *Solanum* and *n* = 3 for *Senecio*) and black points are individual values. Asterisks denote statistical (*p-value* < 0.05) differences between the upper and the basal stems according to Student's t test. Scales = 1 mm. 78

Figure 4. Lignin deposition at the upper and basal regions of the stems of *Solanum lycopersicum* and *Senecio minimus*. Patterns of deposition were assessed by staining the stem cross sections with phloroglucinol, which stains lignin in red. Differences in cell wall residue (CRW) (mg CWR mg dry weight^{-1} x 100) and lignin concentration (mg lignin mg CWR $^{-1}$ x 100). Bars are means ± SE (*n* = 5 for *Solanum* and *n* = 3 for *Senecio*) and black points are individual values. Asterisks denote statistical (*p-value* < 0.05) differences between the upper and the basal stems according to Student's t test. Scales = 500 µm. 79

LIST OF TABLES

CHAPTER 1

Table 1. Leaf area, maximum net CO_2 assimilation rate (A), maximum stomatal conductance to water vapor (g_s), maximum transpiration rate (E), intrinsic water use efficiency (WUE_i), leaf water potential at turgor loss point (Ψ_{TLP}) and minimum leaf conductance (g_{min}) of four tomato genotypes differing in their ability to accumulate foliar ABA: *sitiens (sit)* and *notabilis (not)* are ABA biosynthetic mutants, WT is wild type cv. Ailsa Craig, and *sp12* is a transgenic line over-accumulating ABA. 43

Table 2. Water potential inducing 12% (P_{12}), 50% (P_{50}) and 88% (P_{88}) embolism (optical vulnerability) of leaves and stems or declines in hydraulic conductance of leaves (rehydration kinetics method) of four tomato genotypes differing in their ability to accumulate foliar ABA: *sitiens (sit)* and *notabilis (not)* are ABA biosynthetic mutants, WT is wild type cv. Ailsa Craig, and *sp12* is a transgenic line over-accumulating ABA. 44

Supplemental Table S1. A detailed description of the nutrient solution used for plant cultivation. 50

Supplemental Table S2. Water potential inducing 50% (P_{50}) embolism across leaf vein orders (midrib, secondary and minority veins) of four tomato genotypes differing in their ability to accumulate foliar ABA: *sitiens (sit)* and *notabilis (not)* are ABA biosynthetic mutants, WT is wild type cv. Ailsa Craig, and *sp12* is a transgenic line over-accumulating ABA. 51

CHAPTER 2

Table 1. Water potentials (MPa) at 12, 50, and 88% cumulative embolism (P_{12}, P_{50}, and P_{88}) for leaf, upper stem, and basal stem of *Solanum lycopersicum* and *Senecio minimus*. 73

Table 2. Time for the upper stem to reach critical water potentials (P_{12}, P_{50}, and P_{88}) relative to the basal stem region of *Solanum lycopersicum* and *Senecio minimus*....74

Table 3. Stem area (A_{stem}), xylem area (A_{xylem}), pith area (A_{pith}), xylem vessel diameter (D_h), the xylem cell wall thickness (t) and lumen breadth (b) ratio $(t/b)_3$, and the theoretical stem water flow rate (J_v) for the herbaceous upper stem and the woody basal stem regions of *Solanum lycopersicum* and *Senecio minimus*. 75

Supplemental Table S1. Nutrient solution used for cultivation of *Solanum lycopersicum*.o 80

LIST OF ACRONYMS AND ABBREVIATIONS

A	Photosynthesis
ABA	Abscisic acid
A_{pith}	Pith area
A_{stem}	Stem area
A_{xylem}	Xylem area
b	Lumen breadth
CWR	Cell wall residue
D_h	Hydraulic vessel diameter
D_s	Stomatal density
D_v	Vein density
E	Transpiration
F	Instantaneous flow rate
FOV	Field of view
g_{min}	Minimum leaf conductance
g_s	Stomatal conductance
HSM	Hydraulic safety margin
K	Hydraulic conductance
K_{leaf}	Leaf hydraulic conductance
K_{root}	Root hydraulic conductance
K_{stem}	Stem hydraulic conductance
l	Path lenght
L_s	Stomatal length
n	Sample size
NCED	9-cis-epoxycarotenoid dioxygenase
not	Notabilis tomato mutant
P Xy	Primary xylem
P_{12}	Water potential at 12% cumulative embolism
P_{50}	Water potential at 50% cumulative embolism
P_{88}	Water potential at 88% cumulative embolism
PPFD	Photosynthetic photon flux density
$P_{pith:xylem}$	Pith-to-xylem area ratio
$P_{SecXylem}$	Proportion of secondary xylem vessel to total xylem vessels

S Xy	Secondary xylem
SE	Standard error
sit	Sitiens tomato mutant
soc1	SUPPRESSOR OF OVEREXPRESSION OF CONSTANS 1
sp12	sp12 tomato transgenic
t	Cell wall thickness
(*t*/*b*)3	Cell wall thickness to lumen breadth ratio
V_{leaf}	Water viscosity
VPD	vapor pressure deficit
WT	Wild type
WUE	Water use efficiency
WUE_i	intrinsic water use efficiency
Xy	Xylem

LIST OF SYMBOLS

Ψ_w Plant water potential

Ψ_{leaf} Leaf water potential

Ψ_{TLP} Water potential at turgor loss point

SUMMARY

General introduction 17
References 19
CHAPTER 1 - Abscisic acid acts essentially on stomata, not on xylem, to improve drought tolerance in tomato 22
Abstract 22
Introduction 23
Material and methods 25
Results 31
Discussion 34
Conclusion 37
References 37
Tables 43
Figures 45
Supplementary data 50
CHAPTER 2 - Secondary growth increases embolism resistance in herbaceous plants 55
Abstract 55
Introduction 56
Material and methods 58
Results 62
Discussion 63
Conclusion 67
References 68
Tables 73
Figures 76
Supplementary Material 80
General conclusion 81

GENERAL INTRODUCTION

Water is absorbed from the soil by the roots and then transported throughout the plant via the xylem, eventually reaching the evaporating surfaces present in the leaves where the gas exchange takes place. This remarkable upward movement of water against gravity is made possible by a water potential gradient within the xylem conduits (Dixon & Joly 1895). The risk of xylem dysfunction by embolism intensifies during drought as hydraulic tension within the xylem increases (Tyree & Sperry 1989). Embolism occurs when the negative pressure in the xylem exceeds a threshold, leading to the movement of gas across pit membranes (Tyree & Sperry 1989; Kaack *et al.* 2021; Avila *et al.* 2022). As drought progresses, the spread of embolism throughout the xylem network results in tissue damage and ultimately leads to the mortality of the plant (Urli *et al.* 2013; Hammond *et al.* 2019; Cardoso, Batz & McAdam 2020). Embolism negatively impacts whole-plant function given the declines in the water transport efficiency (i.e., the hydraulic conductance), wherein critical levels of embolism are directly linked to drought-induced mortality (Brodribb & Cochard 2009; Urli *et al.* 2013; Hammond *et al.* 2019). Consequently, the increased resistance to embolism represents an important drought tolerance mechanism that evolved multiple times in land plants (McAdam & Cardoso 2019).

One of the drought tolerance mechanisms that evolved in plants regards the stomata's response to abscisic acid (ABA). Such response allowed seed plants to minimize tissue dehydration and xylem embolism during drought by triggering stomata closure through the accumulation of foliar ABA (Daszkowska-Golec & Szarejko 2013). As water potential declines during drought, so does the turgor (Pierce & Raschke 1980; Creelman & Zeevaart 1985) and volume of leaf cells, triggering the accumulation of ABA primarily in leaves (McAdam & Brodribb 2016; Zhang *et al.* 2018). ABA triggers stomata closure by activating anion channels in the guard cell membrane, actively lowering guard cell turgor (Daszkowska-Golec & Szarejko 2013). The declines in stomatal conductance (g_s) driven by ABA delay the drought-induced plant dehydration and embolism formation, maintaining plants at a safer water potential range (Cardoso, Brodribb, Lucani, DaMatta & McAdam 2018; Creek *et al.* 2020). Notwithstanding, xylem resistance to embolism has been shown to vary enormously across (Choat *et al.* 2012) and within species (Rodriguez-Dominguez, Carins Murphy, Lucani & Brodribb 2018; Cardoso *et al.* 2020; Cardoso, Kane, Rimer & McAdam 2022; Johnson, Lucani

& Brodribb 2022). Research efforts have long focused on exploring the structural traits that are associated with increased stem xylem resistance to embolism (Lens *et al.* 2011, 2022; Levionnois *et al.* 2021; Kaack *et al.* 2021; Johnson & Brodribb 2023). These studies have identified several key variables that associate with increased stem resistance, including narrow xylem conduits with thicker cell walls, thicker pit membranes in interconduit pits, scattered distribution of xylem conduits, lower pith-to-xylem area, and a higher degree of woodiness. Due to technical limitations, however, most of these studies have only assessed woody species, such that the anatomical determinants underlying embolism resistance in herbaceous species remain relatively unknown.

The relative recent development of the optical vulnerability (OV) method has provided scientists with a promising tool to construct vulnerability curves in soft plants (Brodribb, Bienaimé & Marmottant 2016a). The OV method is a relatively cheap, non-invasive, and non-destructive method (when measuring leaf water potential with psychrometers) that captures both timing and real-time propagation of embolism. Indeed, this functionality was essential to demonstrate that xylem embolism in leaves does not occur with open stomata (Creek *et al.* 2020). By using the OV method, several studies have shown that herbs are highly sensitive to cavitation (Skelton, Brodribb & Choat 2017; Ahmad *et al.* 2018; Cardoso *et al.* 2018; Corso *et al.* 2020), and some studies have challenged their ability to refill embolized conduits (Johnson, Jordan & Brodribb 2018). Nevertheless, it has been showed that herbs are not more drought-sensitive than angiosperms trees (Lens *et al.* 2016). However, the mechanisms underlying the drought resistance in herbs, which are crucial for enabling their cultivation in drier environments, remain poorly understood.

Herein, this thesis presents a series of experiments divided into two chapters with the purpose of better understanding the drought mechanisms of herbaceous plants. The first chapter demonstrates that the phytohormone ABA slightly increase leaf xylem embolism resistance, though its primary contribution to drought tolerance is reducing water loss through stomata control. The findings from the first chapter that indicates that older plants have enhanced embolism resistance instigated the main hyphotesis of the next chapter. The second chapter shows that secondary growth in the basal stem of herbs increases xylem resistance to embolism. Together, these findings further our understanding of how hormonal regulation and developmental

processes impact plant hydraulics. The results may help to cultivate herbaceous crops in drier environments.

REFERENCES

Ahmad H.B., Lens F., Capdeville G., Burlett R., Lamarque L.J. & Delzon S. (2018) Intraspecific variation in embolism resistance and stem anatomy across four sunflower (*Helianthus annuus* L.) accessions. *Physiologia Plantarum* **163**, 59–72.

Avila R.T., Guan X., Kane C.N., Cardoso A.A., Batz T.A., DaMatta F.M., … McAdam S.A.M. (2022) Xylem embolism spread is largely prevented by interconduit pit membranes until the majority of conduits are gas-filled. *Plant Cell and Environment* **45**, 1204–1215.

Brodribb T.J., Bienaimé D. & Marmottant P. (2016) Revealing catastrophic failure of leaf networks under stress. *Proceedings of the National Academy of Sciences of the United States of America* **113**, 4865–4869.

Brodribb T.J. & Cochard H. (2009) Hydraulic failure defines the recovery and point of death in water-stressed conifers. *Plant Physiology* **149**, 575–584.

Cardoso A.A., Batz T.A. & McAdam S.A.M. (2020) Xylem embolism resistance determines leaf mortality during drought in *Persea americana*. *Plant Physiology* **182**, 547–554.

Cardoso A.A., Brodribb T.J., Lucani C.J., DaMatta F.M. & McAdam S.A.M. (2018) Coordinated plasticity maintains hydraulic safety in sunflower leaves. *Plant, Cell & Environment* **41**, 2567–2576.

Cardoso A.A., Kane C.N., Rimer I.M. & McAdam S.A.M. (2022) Seeing is believing: what visualising bubbles in the xylem has revealed about plant hydraulic function. *Functional Plant Biology* **49**, 759–772.

Choat B., Jansen S., Brodribb T.J., Cochard H., Delzon S., Bhaskar R., … Zanne A.E. (2012) Global convergence in the vulnerability of forests to drought. *Nature* **491**, 752–755.

Corso D., Delzon S., Lamarque L.J., Cochard H., Torres-Ruiz J.M., King A. & Brodribb T. (2020) Neither xylem collapse, cavitation, or changing leaf conductance drive stomatal closure in wheat. *Plant, Cell & Environment* **43**, 854–865.

Creek D., Lamarque L.J., Torres-Ruiz J.M., Parise C., Burlett R., Tissue D.T. & Delzon S. (2020) Xylem embolism in leaves does not occur with open stomata: Evidence from direct observations using the optical visualization technique. *Journal of Experimental Botany* **71**, 1151–1159.

Creelman R.A. & Zeevaart J.A.D. (1985) Abscisic acid accumulation in spinach leaf slices in the presence of penetrating and nonpenetrating solutes. *Plant Physiology* **77**, 25–28.

Daszkowska-Golec A. & Szarejko I. (2013) Open or close the gate - stomata action under the control of phytohormones in drought stress conditions. *Frontiers in Plant Science* **4**, 1–16.

Dixon H.H. & Joly J. (1895) On the ascent of sap. *Philosophical Transactions of the Royal Society of London. (B.)* **186**, 563–576.

Hammond W.M., Yu K., Wilson L.A., Will R.E., Anderegg W.R.L. & Adams H.D. (2019) Dead or dying? Quantifying the point of no return from hydraulic failure in drought-induced tree mortality. *New Phytologist* **223**, 1834–1843.

Johnson K.M. & Brodribb T.J. (2023) Evidence for a trade-off between growth rate and xylem cavitation resistance in *Callitris rhomboidea*. *Tree Physiology* **00**, 1–11.

Johnson K.M., Jordan G.J. & Brodribb T.J. (2018) Wheat leaves embolized by water stress do not recover function upon rewatering. *Plant, Cell & Environment* **41**, 2704–2714.

Johnson K.M., Lucani C. & Brodribb T.J. (2022) In vivo monitoring of drought-induced embolism in *Callitris rhomboidea* trees reveals wide variation in branchlet vulnerability and high resistance to tissue death. *New Phytologist* **233**, 207–218.

Kaack L., Weber M., Isasa E., Karimi Z., Li S., Pereira L., … Jansen S. (2021) Pore constrictions in intervessel pit membranes provide a mechanistic explanation for xylem embolism resistance in angiosperms. *New Phytologist* **230**, 1829–1843.

Lens F., Gleason S.M., Bortolami G., Brodersen C., Delzon S. & Jansen S. (2022) Functional xylem characteristics associated with drought-induced embolism in angiosperms. *New Phytologist* **236**, 2019–2036.

Lens F., Picon-Cochard C., Delmas C.E.L., Signarbieux C., Buttler A., Cochard H., … Delzon S. (2016) Herbaceous angiosperms are not more vulnerable to drought-induced embolism than angiosperm trees. *Plant Physiology* **172**, 661–667.

Lens F., Sperry J.S., Christman M.A., Choat B., Rabaey D. & Jansen S. (2011) Testing hypotheses that link wood anatomy to cavitation resistance and hydraulic conductivity in the genus Acer. *New Phytologist* **190**, 709–723.

Levionnois S., Jansen S., Wandji R.T., Beauchêne J., Ziegler C., Coste S., … Heuret P. (2021) Linking drought-induced xylem embolism resistance to wood anatomical traits in Neotropical trees. *New Phytologist* **229**, 1453–1466.

McAdam S.A.M. & Brodribb T.J. (2016) Linking turgor with ABA biosynthesis: Implications for stomatal responses to vapor pressure deficit across land plants. *Plant Physiology* **171**, 2008–2016.

McAdam S.A.M. & Cardoso A.A. (2019) The recurrent evolution of extremely resistant xylem. *Annals of Forest Science* **76**, 2–5.

Pierce M. & Raschke K. (1980) Correlation between loss of turgor and accumulation of abscisic acid in detached leaves. *Planta* **148**, 174–182.

Rodriguez-Dominguez C.M., Carins Murphy M.R., Lucani C. & Brodribb T.J. (2018) Mapping xylem failure in disparate organs of whole plants reveals extreme resistance in olive roots. *New Phytologist* **218**, 1025–1035.

Skelton R.P., Brodribb T.J. & Choat B. (2017) Casting light on xylem vulnerability in an herbaceous species reveals a lack of segmentation. *New Phytologist* **214**, 561–569.

Tyree M.T. & Sperry J.S. (1989) Vulnerability of xylem to cavitation and embolism. *Annual Review of Plant Physiology and Plant Molecular Biology* **40**, 19–36.

Urli M., Porté A.J., Cochard H., Guengant Y., Burlett R. & Delzon S. (2013) Xylem embolism threshold for catastrophic hydraulic failure in angiosperm trees. *Tree Physiology* **33**, 672–683.

Zhang F.-P., Sussmilch F., Nichols D.S., Cardoso A.A., Brodribb T.J. & McAdam S.A.M. (2018) Leaves, not roots or floral tissue, are the main site of rapid, external pressure-induced ABA biosynthesis in angiosperms. *Journal of Experimental Botany* **69**, 1261–1267.

CHAPTER 1

Abscisic acid acts essentially on stomata, not on xylem, to improve drought tolerance in tomato

Eduardo J. Haverroth, Leonardo A. Oliveira, Moab T. Andrade, Matthew Taggart, Scott A. M. McAdam, Agustin Zsögön, Andrew J. Thompson, Samuel C.V. Martins, Amanda A. Cardoso[1]

ABSTRACT

Drought resistance is essential for plant production under water-limiting environments. Abscisic acid (ABA) plays a critical role in stomata but its impact on hydraulic function beyond the stomata is far less studied. We selected genotypes differing in their ability to accumulate ABA to investigate its role in drought-induced dysfunction. All genotypes exhibited similar leaf and stem embolism resistance; their leaf hydraulic resistance was also similar. Differences were only observed between the two extreme genotypes: *sitiens* (*sit*; a strong ABA-deficient mutant) and *sp12* (a transgenic line that constitutively over-accumulates ABA), where the water potential inducing 50% embolism was 0.25 MPa lower in *sp12* than in *sit*. Maximum stomatal and minimum leaf conductances were considerably lower in plants with higher ABA (WT and *sp12*) than in ABA-deficient mutants. Variations in gas exchange across genotypes were associated with ABA levels and differences in stomatal density and size. The lower water loss in plants with higher ABA meant that lethal water potentials associated with embolism occurred later during drought in *sp12* plants, followed by WT, and then by the ABA-deficient mutants. Therefore, the primary pathway by which ABA enhances drought tolerance is via declines in water loss, which delays dehydration and hydraulic dysfunction.

INTRODUCTION

Soil drought has been the most detrimental abiotic stress threatening crop production since agricultural emergence in the neolithic period (Lesk, Rowhani & Ramankutty 2016). With ongoing climate changes, even more frequent and severe droughts are predicted to occur in the coming decades, challenging food production in face of an ever-increasing population (Lobell & Field 2007; Dai 2013; Lesk *et al.* 2016). Soil drought impacts different plant processes depending on the level of tissue dehydration. Declines in water content first impair cellular expansion and close stomata limiting CO_2 uptake; then further plant dehydration can lead to extensive damage to the water transport system and ultimately, plant death (Tyree & Sperry 1989; Scoffoni *et al.* 2017; Trueba *et al.* 2019).

For plants to grow and produce, water must be absorbed from the soil by the roots and then transported within the plant through the xylem until it reaches the stomata on the leaf surface. Once in the leaves, water vapor is lost through transpiration (*E*) as the stomata opens to allow the acquisition of CO_2 for photosynthesis (*A*). The ascent of movement of water within the xylem of plants is explained by the “cohesion-tension” theory (Dixon & Joly 1895), where water moves under tension driven by a gradient of water potential (Venturas, Sperry & Hacke 2017). During drought, the risk of xylem dysfunction by embolism increases as the tension in the xylem intensifies (Tyree & Sperry 1989). Cavitation occurs when the xylem tension reaches a threshold at which tiny air bubbles are pulled into the xylem cells. When inside the xylem, the xylem tension causes these bubbles to rapidly expand, blocking the water transport in that specific xylem conduit (i.e. embolism) (Tyree & Sperry 1989).

Embolism negatively impacts whole-plant function given the declines in the water transport efficiency (hydraulic conductance, *K*) that occur when it forms. Consequently, plants that have evolved xylem highly resistant to embolism are likely more tolerant to low water potentials and drought (McAdam and Cardoso, 2019). Xylem resistance to embolism has been shown to vary enormously across (Choat *et al.* 2012) and within species (Rodriguez-Dominguez *et al.* 2018; Cardoso *et al.* 2020, 2022; Johnson *et al.* 2022). Species with narrower xylem vessels are often more resistant to embolism than species with wider conduits (Isasa *et al.* 2023). Similarly, a higher xylem cell wall thickness to lumen breadth ratio has been correlated with a higher embolism resistance (Blackman, Brodribb & Jordan 2010; Cardoso *et al.* 2018),

as well as thicker pit membranes (Dória *et al.* 2018; Thonglim *et al.* 2021, 2023) and a minimally connected xylem network (Loepfe, Martinez-Vilalta, Piñol & Mencuccini 2007; Mrad, Johnson, Love & Domec 2021; Avila *et al.* 2023).

Another mechanism allowing seed plants to minimize tissue dehydration and xylem embolism during drought is through the accumulation of foliar abscisic acid (ABA) and consequent stomatal closure (Daszkowska-Golec & Szarejko 2013). As water potential declines during drought, so does the turgor (Pierce & Raschke 1980; Creelman & Zeevaart 1985) and volume of leaf cells, triggering the accumulation of ABA primarily in leaves (McAdam & Brodribb 2016; Zhang *et al.* 2018). In leaves, the mesophyll is the primary source of drought-induced accumulation of ABA (McAdam & Brodribb 2018). ABA triggers stomata closure by activating anion channels in the guard cell membrane, actively lowering guard cell turgor (Daszkowska-Golec & Szarejko 2013). The declines in stomatal conductance (g_s) driven by ABA delay the drought-induced plant dehydration and embolism formation, maintaining plants at a safer water potential range (Cardoso *et al.* 2018; Creek *et al.* 2020). ABA also (i) improves water use efficiency (WUE) by lowering g_s while maintaining A, (ii) enhances root growth and root hydraulic conductance, and (iii) allows plants to sustain growth during drought (Thompson *et al.* 2007a; Mega *et al.* 2019). The prominent role of ABA in plant function during drought has triggered numerous studies focused on manipulating ABA levels or signal transduction by both chemical (Helander, Vaidya & Cutler 2016) and transgenic approaches (Thompson *et al.* 2007a) aiming at improving WUE and drought resistance in crops.

Recent work has presented evidence that appears to quell hopes for enhancing drought resistance in crops through manipulated increases in ABA levels (Lamarque *et al.* 2020). Lamarque et al. (2020) found that a transgenic line of tomato (*Solanum lycopersicum* L.) that constitutively over-accumulates ABA (*sp12*) exhibits lower (from c. 0.5 to 1.2 MPa) stem xylem resistance to embolism than the WT. In the absence of a drought experiment, however, we are unsure of whether this transgenic ABA line with a less resistant xylem is, in fact, less drought resistant. It is possible that plants over-accumulating ABA exhibit such a conservative mechanism in terms of low water loss, that during drought, plant dehydration is considerably delayed, and plant survival is further prolonged, rendering these plants more drought tolerant than their WT, despite the less resistant xylem to embolism.

In this study, we aimed to better understand the role of ABA in promoting drought resistance through such opposing mechanisms in the xylem and the stomata. We also assessed, for the first time, the impact of ABA on the minimum leaf conductance (g_{min}) – the leaf conductance to water vapor through the cuticle and incompletely closed stomata) (Duursma et al., 2019). To address these gaps, we selected four tomato lines differing in the ability to accumulate ABA. The wild type (WT) cv. Ailsa Craig. Two near-isogenic lines carrying mutations in ABA biosynthesis genes: *sitiens* (*sit*) – deficient in ABA-aldehyde oxidase (Harrison, Burbidge, Okyere, Thompson & Taylor 2011) – and *notabilis* (*not*) – deficient in the rate-limiting enzyme of ABA biosynthesis, 9-*cis*-epoxycarotenoid dioxygenase (NCED) (Burbidge *et al.* 1999). And finally, a transgenic line in the Ailsa Craig genetic background (*sp12*) over-expressing NCED from a constitutive promoter, and thus over-accumulating ABA (Thompson *et al.* 2000, 2007a b). We hypothesized that, despite potential increases in stem xylem resistance to embolism, the primary role of ABA in regulating drought resistance is via stomatal regulation. Plants over-accumulating ABA would be able to delay declines in water potential below the threshold for which embolism and hydraulic dysfunction occur, thus conferring higher drought resistance to this genotype.

MATERIAL AND METHODS

Plant material

Seeds of WT, *sit* and *not* were provided by A. Zsögön (Universidade Federal de Vicosa, Brazil) and seeds of *sp12* were provided by A. Thompson (Cranfield University, UK). Seeds were first germinated in a mixture of 50% Sun Gro Propagation Growing Mix and 50% sand. Germination was considered when both cotyledons had fully emerged, which occurred after c. 20 days for *sp12* and c. five days for *sit*, *not* and WT. Because of the difference in germination time, plants of *sp12* were sowed 15 days prior to the sowing of *sit*, *not* and WT seeds. Therefore, plants were at the same age for all experiments.

One-week seedlings were individually transplanted into 6-L plastic pots containing the substrate aforementioned. Plants were cultivated in an environmentally controlled chamber. Conditions in the chambers were set to 0600:1800 photoperiod with photosynthetic photon flux density (PPFD) of c. 600 µmol m^{-2} s^{-1}, day:night

temperature cycles of 26:22ºC, and ambient levels of CO_2 (c. 420 µmol mol^{-1}). Relative humidity in the chamber was not controlled and ranged from 50 to 70%. Daily irrigation with nutrient solution (Supplementary Table S1) was performed to field capacity until plants achieved 60 days old. Plant age was calculated from the day of emergence. For the following methods, samplings were performed such that less than 20% of the total leaf area of the plants was cut.

Quantification of ABA

The ABA was quantified from healthy and fully expanded leaves from the middle third of the plant shoot (*n* = 6). Sampling was performed in well-watered plants as a means to confirm differences in the intrinsic ability to accumulate ABA across the four genotypes. Samples were weighed, covered in cold (−30°C) 80% (v/v) methanol in water, and immediately stored at −20°C. They were further purified, and the foliar ABA level was quantified by physicochemical methods with an added internal standard using an Agilent 6400 series triple quadrupole LC/MS (Agilent, Santa Clara, United States) according to McAdam (2015). Foliar ABA levels were expressed in terms of dry weight, which was quantified after ABA determination by weighing the dry mass of the sample harvested and extracted for analysis. Normalizing the ABA levels to tissue dry weight avoids passive increases in ABA levels as cells dehydrate.

Optical vulnerability curves

The vulnerability curves of leaves and stems were assessed through the Optical Vulnerability method (Brodribb *et al.* 2016a). Six plants from each genotype (*n* = 6) were brought to the laboratory during the evening, removed from the pots, and had their roots carefully washed. They were maintained overnight with their roots under water with aeration systems to ensure that roots would not suffer from hypoxia. During the next morning, one leaf per plant (the youngest fully expanded leaf) was set up on a microscope (LCD digital microscope; New York Microscope Company, New York, United States) adapted with a bottom light source, while remaining attached to the plant. The leaf was fixed under the microscope using transparent adhesive. From the same plant, we also attached a middle portion of the stem to another microscope. For the stem, the xylem was exposed carefully using a razor blade and then covered with

conductive adhesive gel (Parker Labs, Fairfield, United States) and a cover slip. Images from leaves and stems were taken every 180 s as the plant dehydrated under dark conditions (to induce water potential equilibration throughout the plant), with their roots exposed to air to accelerate plant dehydration. The plant water potential (Ψ_w) was periodically measured using a stem psychrometer (ICT, Armidale, Australia). Leaf water potentials were also measured over time using a pressure chamber to confirm the measurements obtained from the psychrometer. Embolisms were determined by a visible change in color in xylem conduits. The area of embolism was quantified by image subtraction of stacks of images using ImageJ software (National Institutes of Health, Bethesda, United States). Complete descriptive details of this method are available on the open-source website http://www.opensourceov.org. In order to analyze the relationship between plant water potential and embolism formation, a linear regression was fitted between time and Ψ_w, so the Ψ_w of each image could be determined. Mean and standard errors for vulnerability curves were determined every 1% of embolized xylem area and plotted as per (Cardoso *et al.* 2022). The Ψ_w at 12%, 50%, and 88% cumulative embolism (P_{12}, P_{50}, and P_{88}) were obtained for each curve.

Leaf hydraulic vulnerability curves

Leaf hydraulic vulnerability curves describing the declines in leaf hydraulic conductance (K_{leaf}) with dehydration were constructed using the dynamic rehydration kinetics method (Brodribb & Cochard 2009; Blackman & Brodribb 2011). Only fully expanded leaves from the middle third of the plant shoot were utilized. Maximum K_{leaf} was determined from a subset of six well-watered plants (n = 6). Then, plants were allowed to dehydrate due to irrigation withholding and K_{leaf} was determined sequentially by measuring the rehydration flux of water using a hydraulic flowmeter. Before each measurement, a leaf was sampled to determine the minimum leaf water potential (Ψ_{leaf}) to construct the hydraulic curve. Ψ_{leaf} were assessed using a Scholander chamber (Model 1505D, PMS Instruments, Albany, United States). Then a neighboring leaf was excised under water and immediately connected to the flowmeter, where the hydraulic flux into the leaf was logged every 3 s for 60 s or until the flow rate decayed. Subsequently, the leaf was disconnected, bagged, and left to equilibrate for 15 min to measure the final Ψ_{leaf} and leaf area. The initial and final instantaneous K_{leaf} were calculated from the following equation:

$$K_{leaf} = F/(\text{Leaf Area}*\Delta\Psi_w)$$

where F is the instantaneous flow rate into the leaf (F, mmol m^{-2} s^{-1}) and $\Delta\Psi_w$ is the water potential gradient driving the flow, which is equal to final Ψ_{leaf}. Initial and final K_{leaf} were discarded when variation exceeded *c.* 30%. K_{leaf} values were normalized to 25ºC. The relationship between K_{leaf} and initial Ψ_{leaf} were fitted by a three-parameter sigmoidal equation and used to construct the hydraulic vulnerability curve. From each curve, water potentials at 12%, 50%, and 88% of loss in K_{leaf} (P_{12}, P_{50}, and P_{88}) were determined.

Pressure-volume curves and minimum leaf hydraulic conductance

Pressure-volume curves (Tyree & Hammel 1972) were performed using fully expanded, healthy leaves (n = 6). Leaves were sampled and rehydrated overnight to achieve Ψ_{leaf} c. -0.1 MPa. Then, they were allowed to dehydrate on a bench, while mass and Ψ_{leaf} were periodically measured using a digital balance (0.0001 g) and a Scholander chamber. Finally, leaves were placed in an oven at 70°C for at least 48 h to determine the dry mass. Leaf dry weight was used to calculate relative water content, which was plotted against $1/\Psi_{leaf}$. Ψ_{TLP} was estimated as the inflection point of the curve.

The g_{min} was measured according to the mass loss of water from detached leaves method (Duursma et al., 2019). Fully expanded leaves (n = 12) were sampled at pre-dawn and had their petioles covered with parafilm. Next, leaves were scanned for leaf area and weighed immediately using a digital balance to four decimal places. Leaves were then suspended in a growth chamber, allowing slow desiccation. Measurements of leaf mass, temperature, and relative humidity were recorded every 30 min. After reaching water loss stability, leaves were dried at 70°C for at least 48 h and weighed to obtain leaf dry mass. The g_{min} was calculated from the slope of the latter linear region of the relationship between decreasing leaf mass (g) and increasing time (min). This was converted from g^{-1} min^{-1} to mmol m^{-2} s^{-1} by dividing by projected leaf area (m^2) and the mean chamber vapor pressure deficit (VPD), and converting the mass loss from g to mmol H_2O.

Leaf anatomical traits

Leaf anatomical traits were assessed from healthy and fully expanded leaves (*n* = 6) from the middle third of the plant shoot. The following traits were estimated: stomatal density (*Ds*), stomatal length (*Ls*), and vein density (*Dv*). Stomatal measurements were performed on both epidermal sides. Leaves were cleared in 100% methanol for 48 h, followed by incubation in 95% lactic acid at 90ºC until clarification. For each sample, ten fields of view (FOV) were imaged at either 4x or 20x magnification using a digital camera (Zeiss AxioCam HRc, Göttinger, Germany) mounted on a light microscope (AX70 TRF, Olympus Optical, Tokyo, Japan). Measurements were performed using Image-Pro Plus 4.5 (Media Cybernetics, Silver Spring, United States).

Hand-cut transverse sections from fresh stems of 60-day-old plants were also performed. The sections were stained for 5 min with a solution containing phloroglucinol–HCl (1:2) [2% (w:v) phloroglucinol in 95% alcohol and 5 M hydrochloric acid]. Sections were stained with phloroglucinol so that the xylem area could be easily recognized. Images were taken using a digital camera (DP28, Olympus Optical, Tokyo, Japan) mounted on a stereo microscope (ZMS800, Nikon, Japan).

Dry-down experiments

Once the embolism resistances of the genotypes were characterized, dry-down experiments were performed to assess whether the different genotypes would differ in terms of the time taken for plants to reach hydraulic dysfunction during drought (considered here as the mean stem P_{50} of the four genotypes, i.e. -1.30 MPa). In the afternoon before the experiment, a subset of four 60-day-old plants (*n* = 4) were watered until the full substrate capacity. The next day, irrigation was withheld from droughted plants until plants achieved Ψ_w of c. -1.30 MPa, where after plants were irrigated and maintained under well-watered conditions for two additional days. Leaf gas exchange and minimum Ψ_w (measured at midday) were measured daily during the entire experiment. Sampling did not affect more than 20% of the total leaf area per plant. Leaf gas exchange was measured using a Li-6800 (LI-COR, Lincoln, United States) and conditions in the cuvette adjusted accordingly to the growth chamber conditions (PPFD of 600 μmol m^{-2} s^{-1}, 10% of blue light, VPD of 1.5 kPa, and CO_2 at 420 μmol mol^{-1}). The Ψ_w was measured in leaves using a Scholander chamber. On the second day after re-watering, the K_{leaf} was assessed using the evaporative flux method (Brodribb & Holbrook 2006). For this experiment, the evaporative flux method

was selected over the dynamic rehydration kinetics method as leaves had to be sampled and transported from the growth chamber to the laboratory under water. One leaf per plant was collected under water, transported as such to the laboratory and attached to a flowmeter. They were then placed under a PPFD of 1,000 µmol m^{-2} s^{-1} and had the water flow rate logged until flow reached stabilization. Leaves were then allowed to equilibrate for 15 min and had the Ψ_{leaf} measured using a Scholander chamber. The K_{leaf} was calculated from the following equation:

$$K_{leaf} = F*V_{leaf}/(-\Psi_{leaf})$$

where K_{leaf} = leaf hydraulic conductance (mmol m^{-2} s^{-1} MPa^{-1}); V_{leaf} = viscosity of water in the sample leaf relative to 25ºC; and Ψ_{leaf} in MPa. K_{leaf} was normalized by leaf area.

Because of changes in plant morphology (plant height, internode length, and leaf rachis length) across the adult plants of the four genotypes, another dry-down experiment was performed using 20-day-old seedlings (n = 4). These seedlings were young enough to not display changes in plant height and internode length, such that only total leaf area, g_s, and g_{min} would affect the water loss rate and the time for wilting and death. Seedlings were watered to pot capacity and excess water was allowed to drain away. Pots were wrapped with plastic to eliminate soil evaporation and then the pot weight was recorded every minute during dry-down on individual balances accurate to two decimal places. Any mass loss was attributed to the transpiration of soil water. Conditions in the chamber were set to VPD of c. 1.4 kPa (temperature of 20.5 ± 1.5ºC and relative humidity of 41.7 ± 6.9%). The day of visual wilting of all plants per genotype was recorded and the plants remained under drought there until they died (except *sp12* which didn't die even after several days). Seedlings were considered dead when crispy dry. The total leaf area of each plant was measured before the experiment by taking photos of all leaves and measuring leaf area using the ImageJ software. Whole-plant transpiration was then normalized by total leaf area.

We also assessed the hydraulic conductances of leaves (K_{leaf}), stems (K_{stem}), and roots (K_{root}) of 20-day-old seedlings (n = 6). Seedlings were removed from pots and allowed to fully hydrate inside of a glass dome until guttation was observed. An expanded leaf was used to measure K_{leaf} using the evaporative flux method and a hydraulic flowmeter as described earlier (Brodribb & Holbrook 2006). The K_{stem} was obtained gravimetrically (Sperry, Donnelly & Tyree 1988) using entire stem segments (which averaged 6.5 ± 1.5 cm for all genotypes) that were cut under the water. Stems were then attached to a water reservoir containing ultrapure water (type 1) (Millipore

Synergy Ultrapure Water Purification System, Millipore, France) that was placed at different heights (0.2, 0.4, 0.6, 0.8 and 1.0 m) and had the water flow passing through them (mL s^{-1}) measured by a glass micropipette connected to the stem tip. The K_{stem} was estimated as the slope of the flow rate versus the water pressure applied. The K_{root} was measured using an adapted pressure chamber method (Sperry *et al.* 1988; Miyamoto, Steudle, Hirasawa & Lafitte 2001). The roots were immersed in a 50 ml Falcon tube containing ultrapure water (type 1), placed inside a Scholander pressure chamber and connected to a water-filled silicone tube coupled to a precision digital balance (AY 220 model, Shimadzu, Japan). Increasing pressures were applied to the chamber (0.01, 0.02, 0.03, 0.04, and 0.05 MPa) and the flow generated (g s^{-1}) was recorded every 30 s during 150 s. The K_{root} was derived from the slope of the flow rate line versus the water pressure applied.

For leaves, the hydraulic conductance was normalized by leaf area. For stems and roots, the hydraulic conductances were not normalized by stem xylem area or by area or mass of roots. Rather they were simply calculated as the ratio of water flow through the sample to the water potential gradient across the sample (Da-li, Lei, Yu-sen, Feng-wang & Qing-mei 2022). By doing so, we assess hydraulic conductance of the whole organ, taking into account both the inherent hydraulic conductivity of the tissue and differences in organ/tissue size (root surface area, stem length, and xylem area), which ultimately define the total water flux from roots and stems to the leaves.

Statistical analysis

One-way and two-way (data related to the drought experiment) ANOVA was applied in all parameters to test whether the treatments show some difference. When we observed significant effects in ANOVA, multiple mean comparisons were performed using Tukey's posthoc test. All statistical tests and graphics were performed using RStudio (v.4.3.0; Posit Team, 2023).

RESULTS

ABA levels

The differences in ability to accumulate ABA across the four genotypes was confirmed by assessing leaf ABA levels (Table 1). The *sit* (416 ng g^{-1} DW) and *not* (962

ng g^{-1} DW) ABA levels were on average one-fourth and half of the WT levels (1726 ng g^{-1} DW). The *sp12* mean level of ABA (3684 ng g^{-1} DW) was over twice that of the WT.

Embolism resistance of stems and leaves

When stems of young plants (up to 60-day-old) were subjected to dry-down, xylem resistance to embolism was found to be similar across plants of all four genotypes (Table 2; Figure 1), regardless of their ability to accumulate ABA. For all genotypes, embolism initiated (P_{12}) at approximately -1.00 MPa, reached P_{50} between -1.30 and -1.45 MPa, and reached 88% of xylem embolism (P_{88}) between -1.50 and -1.75 MPa (Table 2). Higher variation in xylem resistance within genotype was observed for WT and *sp12* plants than for the two ABA-mutants, *sit* and *not* (Figure 1).

The leaf P_{12} and P_{88} were similar across genotypes as observed by the optical and hydraulic methods (Table 2, Figure 2, Figure 3). Differences were observed for the mean P_{50} values of leaves. Similar P_{50} was observed for *not*, the least severe ABA-deficient mutant, WT, and the ABA-over-accumulating line *sp12*. The most severe ABA deficient mutant, *sit*, exhibited leaves with xylem that was significantly less resistant to embolism than *sp12*, as observed by the optical (a difference of -0.24 MPa, *p*-value = 0.03) and the hydraulic method (a difference of -0.18 MPa, *p*-value = 0.04). In all genotypes, the embolism in the leaf xylem started in the midrib and quickly spread to the higher vein orders (Figure 2; Supplementary Table 2). The hydraulic safety margin (HSM), calculated as the difference between the water potential at the turgor loss point (Ψ_{TLP}) and P_{50} in leaves also differed across genotypes, with the two ABA-deficient mutants exhibiting lower HSM (0.37 MPa for *sit* and 0.34 for *not*) than WT (0.54 MPa) and *sp12* (0.52 MPa) (Figure 2). The higher HSM observed for WT plants over the ABA-deficient mutants resulted from its higher Ψ_{TLP} (Table 1).

Overall, changes in Ψ_{TLP} across genotypes were not consistent with the constitutive levels of foliar ABA (Table 1). *Sit*, WT, and *sp12* had similar Ψ_{TLP} as well as *sit*, *not*, and *sp12*. The only difference in Ψ_{TLP} occurred between *not* (-1.04 MPa) and WT (-0.84 MPa).

Maximum and minimum stomatal conductances

Given the contrasting constitutive levels of ABA biosynthesis across the four genotypes, differences in the leaf gas exchange rate between these plants were observed under well-watered conditions (Table 1). Maximum g_s was dependent on the constitutive levels of foliar ABA, such that *sit* mutant plants achieved the highest g_s (1.76 mol m^{-2} s^{-1}), followed by plants of *not* (1.01 mol m^{-2} s^{-1}), WT (0.57 mol m^{-2} s^{-1}), and finally *sp12* (0.35 mol m^{-2} s^{-1}). Changes in g_s translated into changes in *E*, but we observed no differences in *A* across genotypes. Consequently, the WUE_i (calculated as A/g_s) was highest in *sp12* (c. 55) and significantly higher than that of the two ABA-deficient mutant lines (10.20 in *sit* and c. 19 in *not*). Substantial changes in g_{min} were also observed across genotypes, with plants of WT and *sp12* exhibiting the lowest values of g_{min} (6.6 and 4.2 mmol m^{-2} s^{-1}, respectively), followed by plants of *not* (20.2 mmol m^{-2} s^{-1}), and last by *sit* (28.1 mmol m^{-2} s^{-1}). The g_{min} of *not* and *sit* mutant plants were approximately five and seven times that of *sp12* mutant plants, respectively.

Changes in maximum g_s and g_{min} due to genotype differences in ABA biosynthesis were not only caused by a change in stomatal aperture but also by changes in stomatal anatomy (Supplementary Figure S1). The *sit* plants exhibited higher stomatal density on both leaf surfaces when compared to WT plants. Besides having more stomata per leaf area, the stomata of *sit* mutant plants were also larger than that of the other genotypes. On the other extreme, *sp12* mutant plants exhibited lower stomatal densities than plants of the other genotypes.

Dry-down experiments and time to reach critical water potential

Following water withholding, mature (60-day-old) plants of all genotypes decreased Ψ_{leaf} and g_s (Figure 4). Plants were allowed to dry until the critical Ψ_{leaf} of c. -1.30 MPa, which was selected because of a close proximity with the mean stem P_{50} of plants of *sit*, *not*, and WT. The time for plants to reach this critical threshold was substantially different across genotypes: five, six, nine, and twelve days for *not*, *sit*, WT, and *sp12* plants, respectively (Figure 4A). Note that the total leaf area per plant was similar across droughted plants from all genotypes (Figure 4D). Plants of WT and *sp12* had tightly closed stomata by the time plants reached the critical Ψ_{leaf}, while *sit* and *not* mutant plants continued to exhibit relatively high g_s (Figure 4B). Plants from all genotypes showed visible wilting at the critical Ψ_{leaf}, and the leaf water turgor could recover after re-watering (Supplemental Figure S2). They also displayed limited

recovery in K_{leaf} even after two days of re-watering (Figure 4C), indicating that embolism in leaf xylem had occurred. Decreases in K_{leaf} were 58%, 51%, 50%, and 41% for plants of *sit*, *not*, WT, and *sp12*, respectively.

The dry-down experiment with seedlings demonstrated that plants of the two ABA-deficient mutants wilted and died before the WT (Figure 5). The *sit* seedlings were the first to wilt (at day five), despite having the lowest total leaf area. Plants of *not*, WT, and *sp12* wilted at days eleven, fourteen, and sixteen after water withholding. Plants of *sp12* were the only ones alive after 18 days without irrigation. Seedlings of *not*, WT, and *sp12* had similar K_{leaf}, K_{stem}, and K_{root}. The *sit* plants exhibited lower K_{stem} than *not* and lower K_{root} than WT plants.

DISCUSSION

Our findings demonstrate that the embolism resistances of stems and leaves are essentially similar across young plants of tomato with different abilities to accumulate ABA. In contrast to the minor effect of ABA levels on the xylem physiology, our findings reinforce the critical role of ABA in reducing maximum g_s and demonstrate for the first time its effect on lowering g_{min}, thus improving WUE during well-watered conditions and delaying plant dehydration and damage during drought.

ABA levels and xylem embolism resistance

Our results show that the internal levels of ABA do not impact the embolism resistance of stems of young (60 days old) plants of tomato in a similar way to what was observed for very old (170-day-old) plants (Lamarque *et al.* 2020). This result contrasts with the negative impact of increased ABA levels on the stem embolism resistance of tomato plants at 90 and 120 days old (Lamarque et al., 2020). Therefore, the decreases in embolism resistance in over-accumulating ABA plants appear to only occur during part of the plant life cycle, which might be associated with differences in stem anatomy throughout the plant development.

In our study, the 60-day-old plants from all four genotypes were at a similar stage of secondary growth (Supplemental Figure S3). At this age, stems from all genotypes had started transitioning from primary to secondary growth, and they showed similar areas of secondary xylem. In the case of Lamarque et al. (2020),

images of stems of 120-day-old plants of *sp12* and WT obtained by micro-CT show that the WT plants exhibited a much more developed secondary xylem than the *sp12* plants at the time that the experiment was conducted, which might have been caused by the increased constitutive levels of ABA. Stems of older plants of tomato have long been known to exhibit secondary growth, with a higher proportion of secondary xylem (often named wood), and a higher degree of lignification than younger plants (Thompson & Heimsch 1964). Such increased degree in woodiness and lignification has previously been associated with increased xylem resistance to embolism in stems of herbaceous plants that can develop secondary xylem (Dória *et al.* 2018, 2019; Thonglim *et al.* 2021, 2023). In very old (170 days old) tomato plants of WT and *sp12*, in which similar stem xylem resistances were observed (Lamarque et al., 2020), a complete transition to secondary growth is likely to have occurred.

A number of studies demonstrate that increased ABA levels associate with vascular cambium dormancy in woody species (Fromm, 1997; Mwange et al., 2005; Hou et al., 2006; Ding et al., 2016), thus supporting our hypothesis of delayed secondary xylem development in plants of *sp12* over the WT. In any case, further experiments thoroughly assessing the transition from primary to secondary growth of ABA mutants and over-accumulating ABA lines are necessary to confirm whether ABA delays the formation of secondary xylem in herbaceous plants.

Increased ABA biosynthesis was also essentially disconnected from leaf embolism resistance. A marginal increase (0.24 MPa) in P_{50} was only observed when comparing genotypes with the extremes of ABA level (*sp12* versus *sit* mutant plants). The same increase was not observed for P_{12} and P_{88}. This result is not surprising given the absence of secondary xylem development in leaves.

ABA reduces water loss and delays plant dehydration

The over-accumulation of ABA resulted in partially closed stomata, and thus in lower water loss from leaves to the atmosphere. Given that photosynthesis was not affected, *sp12* mutant plants operated at elevated WUE, as previously reported by Thompson et al. (2007a) through gas exchange, gravimetric, and carbon isotope discrimination methods. The over-accumulation of ABA also resulted in very low minimum leaf conductance likely due to lower stomatal density and size (Muchow & Sinclair 1989; Machado *et al.* 2021). Even though declines in stomatal density have

been previously associated with higher ABA levels – likely due to increased cell turgor and growth (Xie *et al.* 2006; Tanaka, Nose, Jikumaru & Kamiya 2013), this is the first time, to the best of our knowledge, that increased ABA levels are associated with lower minimum leaf conductance. Low minimum leaf conductance is of paramount importance for plants to minimize residual transpiration after stomatal closure and delay further dehydration below thresholds of hydraulic and photosynthetic damage (Gleason, Blackman, Cook, Laws & Westoby 2014; Duursma *et al.* 2019).

Due to changes in maximum and minimum stomatal conductances, genotypes with contrasting ABA levels reached the same critical water potential after very different times. This demonstrates that not only the water potential inducing embolism and damage is important but also the time needed by plants to reach those threshold water potentials (Blackman *et al.* 2019). Another important component influencing dehydration time is the total leaf area per plant and the leaf distribution across the plant (plant architecture), both influencing the total water loss (Blackman *et al.* 2019). At the same time, the hydraulic conductances of leaves, stems, and roots limit the water supply to the leaves, thus buffering water loss to the atmosphere and plant dehydration.

For the dry-down of adult plants, the higher leaf area in *not* compared to *sit* mutant plants might explain why *not* mutant plants reached the critical water potential of -1.30 MPa before *sit* mutant plants, despite lower minimum rates of conductance in *not* over *sit* plants. Besides, adult plants of the *sit* mutant exhibited curled leaves and shorter internodes (Table1) (Stubbe 1957, 1958), and such modifications in plant architecture might have also contributed to a delayed dehydration in this genotype. For the dry-down of seedlings, *sit* plants reached turgor loss point before *not* plants, despite the lower total leaf area. This might have been driven by its substantially higher evaporation rate per unit area, as well as by a potentially lower water flux from roots and stems to the leaves (Figure 5). ABA-deficient mutants are known to have low K_{root} (Tal and Nevo, 1973), and the combination of low K_{root} and inability to close stomata would inevitably lead to rapid wilting in drying soil or high VPD. In other studies, *sp12* was reported to have higher K_{root} than WT, consistent with a positive relationship between ABA level and K_{root} (Thompson *et al.* 2007a). In the case of *not*, *WT*, and *sp12* plants, changes in time were found despite similar total leaf areas and hydraulic conductances, likely due to changes in maximum and minimum stomatal conductances.

CONCLUSION

The impact of ABA on drought tolerance in young plants of tomato is essentially associated with stomatal function, and not with xylem resistance to embolism. Leaves and stems of genotypes spanning a large variation in the constitutive levels of ABA have essentially similar embolism resistance, which does not seem to occur throughout the plant life cycle (Lamarque et al., 2020). Genotypes with higher constitutive levels of ABA have lower maximum stomatal and minimum leaf conductances, efficiently improving WUE under well-watered conditions and delaying hydraulic dysfunction and damage during drought. Given that tomato plants are often cultivated with supplemental irrigation, improvements in water conservation resulting from increased amounts of ABA are likely more important for agriculture than the potential declines in embolism resistance during part of the plant life cycle. We still lack, however, studies assessing the impact of ABA on plant productivity, such that genotypes over-accumulating ABA can finally be used in agriculture.

Acknowledgments

This study was supported by the USDA National Institute of Food and Agriculture, Hatch Project 7003279 (AAC) and the National Science Foundation grant IOS-2140119 (SAMM). The authors acknowledge the use of Bindley Bioscience Center at Purdue University (National Institutes of Health-funded Indiana Clinical and Translational Sciences Institute), particularly the Metabolite Profiling Facility.

REFERENCES

Avila R.T., Kane C.N., Batz T.A., Trabi C., Damatta F.M., Jansen S. & McAdam S.A.M. (2023) The relative area of vessels in xylem correlates with stem embolism resistance within and between genera. *Tree Physiology* **43**, 75–87.

Blackman C.J. & Brodribb T.J. (2011) Two measures of leaf capacitance: insights into the water transport pathway and hydraulic conductance in leaves. *Functional Plant Biology* **38**, 118.

Blackman C.J., Brodribb T.J. & Jordan G.J. (2010) Leaf hydraulic vulnerability is related to conduit dimensions and drought resistance across a diverse range of woody angiosperms. *New Phytologist* **188**, 1113–1123.

Blackman C.J., Li X., Choat B., Rymer P.D., de Kauwe M.G., Duursma R.A., … Medlyn B.E. (2019) Desiccation time during drought is highly predictable across species of *Eucalyptus* from contrasting climates. *New Phytologist* **224**, 632–643.

Brodribb T.J. & Cochard H. (2009) Hydraulic failure defines the recovery and point of death in water-stressed conifers. *Plant Physiology* **149**, 575–584.

Brodribb T.J. & Holbrook N.M. (2006) Declining hydraulic efficiency as transpiring leaves desiccate: Two types of response. *Plant, Cell and Environment* **29**, 2205–2215.

Brodribb T.J., Bienaimé D. & Marmottant P. (2016) Revealing catastrophic failure of leaf networks under stress. *Proceedings of the National Academy of Sciences of the United States of America* **113**, 4865–4869.

Burbidge A., Grieve T.M., Jackson A., Thompson andrew, McCarty D.R. & Taylor I.B. (1999) Characterization of the ABA-deficient tomato mutant *notabilis* and its relationship with maize *Vp14*. *The Plant Journal* **17**, 427–431.

Cardoso A.A., Batz T.A. & McAdam S.A.M. (2020) Xylem embolism resistance determines leaf mortality during drought in *Persea americana*. *Plant Physiology* **182**, 547–554.

Cardoso A.A., Brodribb T.J., Lucani C.J., DaMatta F.M. & McAdam S.A.M. (2018) Coordinated plasticity maintains hydraulic safety in sunflower leaves. *Plant, Cell & Environment* **41**, 2567–2576.

Cardoso A.A., Kane C.N., Rimer I.M. & McAdam S.A.M. (2022) Seeing is believing: what visualising bubbles in the xylem has revealed about plant hydraulic function. *Functional Plant Biology* **49**, 759–772.

Choat B., Brodribb T.J., Brodersen C.R., Duursma R.A., López R. & Medlyn B.E. (2018) Triggers of tree mortality under drought. *Nature* **558**, 531–539.

Choat B., Jansen S., Brodribb T.J., Cochard H., Delzon S., Bhaskar R., … Zanne A.E. (2012) Global convergence in the vulnerability of forests to drought. *Nature* **491**, 752–755.

Creek D., Lamarque L.J., Torres-Ruiz J.M., Parise C., Burlett R., Tissue D.T. & Delzon S. (2020) Xylem embolism in leaves does not occur with open stomata: Evidence from direct observations using the optical visualization technique. *Journal of Experimental Botany* **71**, 1151–1159.

Creelman R.A. & Zeevaart J.A.D. (1985) Abscisic acid accumulation in spinach leaf slices in the presence of penetrating and nonpenetrating solutes. *Plant Physiology* **77**, 25–28.

Dai A. (2013) Increasing drought under global warming in observations and models. *Nature Climate Change* **3**, 52–58.

Da-li G., Lei L., Yu-sen Y., Feng-wang M. & Qing-mei G. (2022) Factors affecting hydraulic conductivity and methods to measure in plants. *Journal of Integrative Agriculture* **21**, 310–315.

Daszkowska-Golec A. & Szarejko I. (2013) Open or close the gate - stomata action under the control of phytohormones in drought stress conditions. *Frontiers in Plant Science* **4**, 1–16.

Ding, Q., Zeng, J., & He, X. Q. (2016). MiR169 and its target PagHAP2-6 regulated by ABA are involved in poplar cambium dormancy. Journal of plant physiology, 198, 1-9.

Dixon H.H. & Joly J. (1895) On the ascent of sap. *Philosophical Transactions of the Royal Society of London. (B.)* **186**, 563–576.

Dória L.C., Meijs C., Podadera D.S., del Arco M., Smets E., Delzon S. & Lens F. (2019) Embolism resistance in stems of herbaceous Brassicaceae and Asteraceae is linked to differences in woodiness and precipitation. *Annals of Botany* **124**, 1–14.

Dória L.C., Podadera D.S., Arco M., Chauvin T., Smets E., Delzon S. & Lens F. (2018) Insular woody daisies (*Argyranthemum*, Asteraceae) are more resistant to drought-induced hydraulic failure than their herbaceous relatives. *Functional Ecology* **32**, 1467–1478.

Duursma R.A., Blackman C.J., Lopéz R., Martin-StPaul N.K., Cochard H. & Medlyn B.E. (2019) On the minimum leaf conductance: its role in models of plant water use, and ecological and environmental controls. *New Phytologist* **221**, 693–705.

Fromm J (1997) Hormonal physiology of wood growth in willow (Salix viminalis L.): effects of spermine and abscisic acid. Wood Sci Technol 31:119–130

Gleason S.M., Blackman C.J., Cook A.M., Laws C.A. & Westoby M. (2014) Whole-plant capacitance, embolism resistance and slow transpiration rates all contribute to longer desiccation times in woody angiosperms from arid and wet habitats. *Tree Physiology* **34**, 275–284.

Harrison E., Burbidge A., Okyere J.P., Thompson A.J. & Taylor I.B. (2011) Identification of the tomato ABA-deficient mutant *sitiens* as a member of the ABA-aldehyde oxidase gene family using genetic and genomic analysis. *Plant Growth Regulation* **64**, 301–309.

Helander J.D.M., Vaidya A.S. & Cutler S.R. (2016) Chemical manipulation of plant water use. *Bioorganic and Medicinal Chemistry* **24**, 493–500.

Hou H-W, Zhou Y-T, Mwange K-N, Li W-F, He X-Q, Cui K-M (2006) ABP1 expression regulated by IAA and ABA is associated with the cambium periodicity in Eucommia ulmoides Oliv. J Exp Bot 57: 3857–3867.

Isasa E., Link R.M., Jansen S., Tezeh F.R., Kaack L., Sarmento Cabral J. & Schuldt B. (2023) Addressing controversies in the xylem embolism resistance–vessel diameter relationship. *New Phytologist*.

Johnson K.M., Lucani C. & Brodribb T.J. (2022) In vivo monitoring of drought-induced embolism in *Callitris rhomboidea* trees reveals wide variation in branchlet vulnerability and high resistance to tissue death. *New Phytologist* **233**, 207–218.

Lamarque L.J., Delzon S., Toups H., Gravel A.I., Corso D., Badel E., … Gambetta G.A. (2020) Over-accumulation of abscisic acid in transgenic tomato plants increases the risk of hydraulic failure. *Plant Cell and Environment* **43**, 548–562.

Lesk C., Rowhani P. & Ramankutty N. (2016) Influence of extreme weather disasters on global crop production. *Nature* **529**, 84–87.

Lobell D.B. & Field C.B. (2007) Global scale climate-crop yield relationships and the impacts of recent warming. *Environmental Research Letters* **2**.

Loepfe L., Martinez-Vilalta J., Piñol J. & Mencuccini M. (2007) The relevance of xylem network structure for plant hydraulic efficiency and safety. *Journal of Theoretical Biology* **247**, 788–803.

Machado R., Loram-Lourenço L., Farnese F.S., Alves R.D.F.B., Sousa L.F., Silva F.G., … Menezes-Silva P.E. (2021) Where do leaf water leaks come from? Trade-offs underlying the variability in minimum conductance across tropical savanna species with contrasting growth strategies. *New Phytologist* **229**, 1415–1430.

McAdam S. (2015) Physicochemical quantification of abscisic acid levels in plant tissues with an added internal standard by ultra-performance liquid chromatography. *Bio-Protocol* **5**, e1599–e1612.

McAdam S.A.M. & Brodribb T.J. (2016) Linking turgor with ABA biosynthesis: Implications for stomatal responses to vapor pressure deficit across land plants. *Plant Physiology* **171**, 2008–2016.

McAdam S.A.M. & Brodribb T.J. (2018) Mesophyll cells are the main site of abscisic acid biosynthesis in water-stressed leaves. *Plant Physiology* **177**, 911–917.

McAdam S.A.M. & Cardoso A.A. (2019) The recurrent evolution of extremely resistant xylem. *Annals of Forest Science* **76**, 1-4

Mega R., Abe F., Kim J.S., Tsuboi Y., Tanaka K., Kobayashi H., … Okamoto M. (2019) Tuning water-use efficiency and drought tolerance in wheat using abscisic acid receptors. *Nature Plants* **5**, 153–159.

Miyamoto N., Steudle E., Hirasawa T. & Lafitte R. (2001) Hydraulic conductivity of rice roots. *Journal of Experimental Botany* **52**, 1835–1846.

Mrad A., Johnson D.M., Love D.M. & Domec J. (2021) The roles of conduit redundancy and connectivity in xylem hydraulic functions. *New Phytologist* **231**, 996–1007.

Muchow R.C. & Sinclair T.R. (1989) Epidermal conductance, stomatal density and stomatal size among genotypes of *Sorghum bicolor* (L.) Moench. *Plant, Cell and Environment* **12**, 425–431.

Mwange, K. N. K., Hou, H. W., Wang, Y. Q., He, X. Q., & Cui, K. M. (2005). Opposite patterns in the annual distribution and time-course of endogenous abscisic acid and indole-3-acetic acid in relation to the periodicity of cambial activity in Eucommia ulmoides Oliv. Journal of experimental botany, 56(413), 1017-1028.

Pierce M. & Raschke K. (1980) Correlation between loss of turgor and accumulation of abscisic acid in detached leaves. *Planta* **148**, 174–182.

Posit Team (2023) RStudio: Integrated Development Environment for R.

Rodriguez-Dominguez C.M., Carins Murphy M.R., Lucani C. & Brodribb T.J. (2018) Mapping xylem failure in disparate organs of whole plants reveals extreme resistance in olive roots. *New Phytologist* **218**, 1025–1035.

Scoffoni C., Albuquerque C., Brodersen C.R., Townes S. V., John G.P., Bartlett M.K., … Sack L. (2017) Outside-xylem vulnerability, not xylem embolism, controls leaf hydraulic decline during dehydration. *Plant Physiology* **173**, 1197–1210.

Sperry J.S., Donnelly J.R. & Tyree M.T. (1988) A method for measuring hydraulic conductivity and embolism in xylem. *Plant, Cell and Environment* **11**, 35–40.

Stubbe H. (1957) Mutanten der kultur tomate *Lycopersicon esculentum* Miller I. *Die Kulturpflanze* **5**, 190–220.

Stubbe H. (1958) Mutanten der kultur tomate *Lycopersicon esculentum* Miller II. *Die Kulturpflanze* **6**, 89–115.

Tal M. & Nevo Y. (1973) Abnormal stomatal behavior and root resistance, and hormonal imbalance in three wilty mutants of tomato. *Biochemical Genetics* **8**, 291–300.

Tanaka Y., Nose T., Jikumaru Y. & Kamiya Y. (2013) ABA inhibits entry into stomatal-lineage development in Arabidopsis leaves. *The Plant Journal* **74**, 448–457.

Thompson A.J., Andrews J., Mulholland B.J., McKee J.M.T., Hilton H.W., Horridge J.S., … Taylor I.B. (2007a) Overproduction of abscisic acid in tomato increases transpiration efficiency and root hydraulic conductivity and influences leaf expansion. *Plant Physiology* **143**, 1905–1917.

Thompson A.J., Jackson A.C., Symonds R.C., Mulholland B.J., Dadswell A.R., Blake P.S., … Taylor I.B. (2000) Ectopic expression of a tomato 9-cis-epoxycarotenoid dioxygenase gene causes over-production of abscisic acid. *Plant Journal* **23**, 363–374.

Thompson A.J., Mulholland B.J., Jackson A.C., McKee J.M.T., Hilton H.W., Symonds R.C., … Taylor I.B. (2007b) Regulation and manipulation of ABA biosynthesis in roots. *Plant, Cell and Environment* **30**, 67–78.

Thompson N.P. & Heimsch C. (1964) Stem anatomy and aspects of development in tomato. *American Journal of Botany* **51**, 7–19.

Thonglim A., Bortolami G., Delzon S., Larter M., Offringa R., Keurentjes J.J.B., … Lens F. (2023) Drought response in Arabidopsis displays synergistic coordination between stems and leaves. *Journal of Experimental Botany* **74**, 1004–1021.

Thonglim A., Delzon S., Larter M., Karami O., Rahimi A., Offringa R., … Lens F. (2021) Intervessel pit membrane thickness best explains variation in embolism resistance amongst stems of *Arabidopsis thaliana* accessions. *Annals of Botany* **128**, 171–182.

Trueba S., Pan R., Scoffoni C., John G.P., Davis S.D. & Sack L. (2019) Thresholds for leaf damage due to dehydration: declines of hydraulic function, stomatal conductance and cellular integrity precede those for photochemistry. *New Phytologist* **223**, 134–149.

Tyree M.T. & Hammel H.T. (1972) The measurement of the turgor pressure and the water relations of plants by the pressure-bomb technique. *Journal of Experimental Botany* **23**, 267–282.

Tyree M.T. & Sperry J.S. (1989) Vulnerability of xylem to cavitation and embolism. *Annual Review of Plant Physiology and Plant Molecular Biology* **40**, 19–36.

Venturas M.D., Sperry J.S. & Hacke U.G. (2017) Plant xylem hydraulics: What we understand, current research, and future challenges. *Journal of Integrative Plant Biology* **59**, 356–389.

Xie X., Wang Y., Williamson L., Holroyd G.H., Tagliavia C., Murchie E., … Hetherington A.M. (2006) The identification of genes involved in the stomatal response to reduced atmospheric relative humidity. *Current Biology* **16**, 882–887.

Zhang F.-P., Sussmilch F., Nichols D.S., Cardoso A.A., Brodribb T.J. & McAdam S.A.M. (2018) Leaves, not roots or floral tissue, are the main site of rapid, external pressure-induced ABA biosynthesis in angiosperms. *Journal of Experimental Botany* **69**, 1261–1267.

TABLES

Table 1. Leaf area, maximum net CO_2 assimilation rate (*A*), maximum stomatal conductance to water vapor (g_s), maximum transpiration rate (*E*), intrinsic water use efficiency (WUE_i), leaf water potential at turgor loss point (Ψ_{TLP}) and minimum leaf conductance (g_{min}) of four tomato genotypes differing in their ability to accumulate foliar ABA: *sitiens (sit)* and *notabilis (not)* are ABA biosynthetic mutants, WT is wild type cv. Ailsa Craig, and *sp12* is a transgenic line over-accumulating ABA.

Trait	*n*	*sit*	*not*	WT	*sp12*
Foliar ABA (ng g^{-1} DW)	6	416 ± 26^{c}	962 ± 167^{bc}	1726 ± 131^{b}	3684 ± 634^{a}
Plant leaf area (m^2)	4	0.15 ± 0.03^{b}	0.20 ± 0.01^{a}	0.23 ± 0.01^{a}	0.23 ± 0.03^{a}
A (µmol CO_2 m^{-2} s^{-1})	8	17.63 ± 1.36^{a}	18.58 ± 0.93^{a}	17.77 ± 1.29^{a}	16.21 ± 1.58^{a}
g_s (mol H_2O m^{-2} s^{-1})	8	1.76 ± 0.15^{a}	1.01 ± 0.04^{b}	0.57 ± 0.12^{c}	0.35 ± 0.06^{d}
E (mmol H_2O m^{-2} s^{-1})	8	17.39 ± 0.52^{a}	14.43 ± 0.42^{ab}	10.95 ± 1.48^{b}	6.98 ± 0.91^{c}
WUE_i (A/g_s)	8	10.20 ± 0.61^{c}	18.54 ± 0.83^{bc}	40.31 ± 8.57^{ab}	54.97 ± 7.94^{a}
Ψ_{TLP} (MPa)	6	-0.99 ± 0.08^{ab}	-1.04 ± 0.01^{b}	-0.84 ± 0.02^{a}	-0.99 ± 0.01^{ab}
g_{min} (mmol H_2O m^{-2} s^{-1})	12	28.10 ± 2.06^{a}	20.70 ± 1.68^{b}	6.66 ± 0.95^{c}	4.24 ± 0.48^{c}

Data are mean ± standard error (*n* is described to each trait). Superscript letters denote results from statistical tests (Tukey, $p<0.05$) conducted between genotypes.

Table 2. Water potential inducing 12% (P_{12}), 50% (P_{50}) and 88% (P_{88}) embolism (optical vulnerability) of leaves and stems or declines in hydraulic conductance of leaves (rehydration kinetics method) of four tomato genotypes differing in their ability to accumulate foliar ABA: *sitiens (sit)* and *notabilis (not)* are ABA biosynthetic mutants, WT is wild type cv. Ailsa Craig, and *sp12* is a transgenic line over-accumulating ABA.

Trait	*sit*	*not*	WT	*sp12*
Leaf Optical Vulnerability				
P_{12} (MPa)	-1.04 ± 0.07^{a}	-1.09 ± 0.09^{a}	-1.04 ± 0.06^{a}	-1.01 ± 0.05^{a}
P_{50} (MPa)	-1.27 ± 0.03^{a}	-1.38 ± 0.03^{ab}	-1.38 ± 0.06^{ab}	-1.51 ± 0.03^{b}
P_{88} (MPa)	-1.40 ± 0.06^{a}	-1.50 ± 0.04^{ab}	-1.74 ± 0.12^{b}	-1.63 ± 0.07^{ab}
Stem Optical Vulnerability				
P_{12} (MPa)	-1.04 ± 0.07^{a}	-1.04 ± 0.03^{a}	-1.10 ± 0.08^{a}	-0.93 ± 0.10^{a}
P_{50} (MPa)	-1.35 ± 0.07^{a}	-1.33 ± 0.03^{a}	-1.47 ± 0.08^{a}	-1.33 ± 0.09^{a}
P_{88} (MPa)	-1.48 ± 0.08^{a}	-1.48 ± 0.03^{a}	-1.75 ± 0.15^{a}	-1.69 ± 0.13^{a}
Rehydration kinetics Method				
P_{12} (MPa)	-1.21 ± 0.10^{a}	-1.21 ± 0.06^{a}	-1.27 ± 0.06^{a}	-1.29 ± 0.11^{a}
P_{50} (MPa)	-1.30 ± 0.03^{a}	-1.33 ± 0.03^{ab}	-1.42 ± 0.06^{ab}	-1.48 ± 0.05^{b}
P_{88} (MPa)	-1.50 ± 0.04^{a}	-1.45 ± 0.05^{a}	-1.50 ± 0.06^{a}	-1.66 ± 0.06^{a}

Data are mean ± standard error (n = 6). Superscript letters denote results from statistical tests (Tukey, p<0.05) conducted between genotypes.

FIGURES

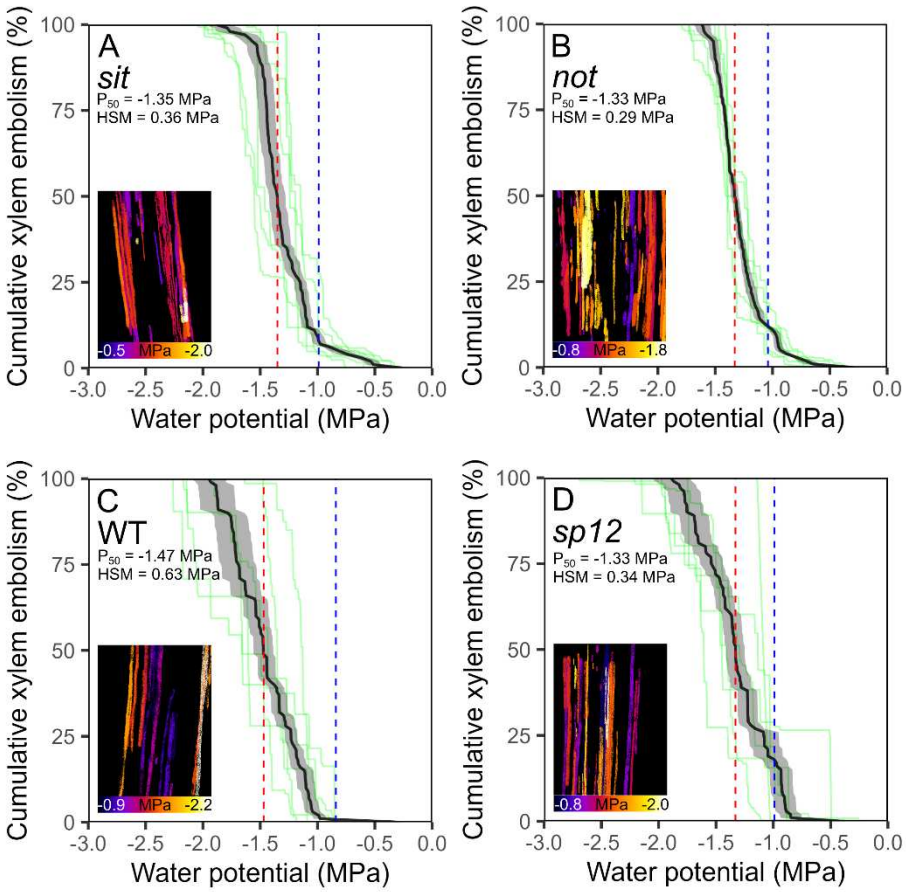

Figure 1. Stem xylem vulnerability curves obtained from the optical vulnerability technique of four tomato genotypes differing in their ability to accumulate foliar ABA: *sitiens (sit)* and *notabilis (not)* are ABA biosynthetic mutants, WT is wild type cv. Ailsa Craig, and *sp12* is a transgenic line over-accumulating ABA. Black line and shadow represent means and standard errors (n = 6), respectively. Green lines are replicates. Blue dashed lines represent leaf turgor loss points and red dashed lines indicate the water potentials associated with 50% of cumulative stem xylem embolism (P_{50}). The difference between these two parameters is the hydraulic safety margin (HSM).

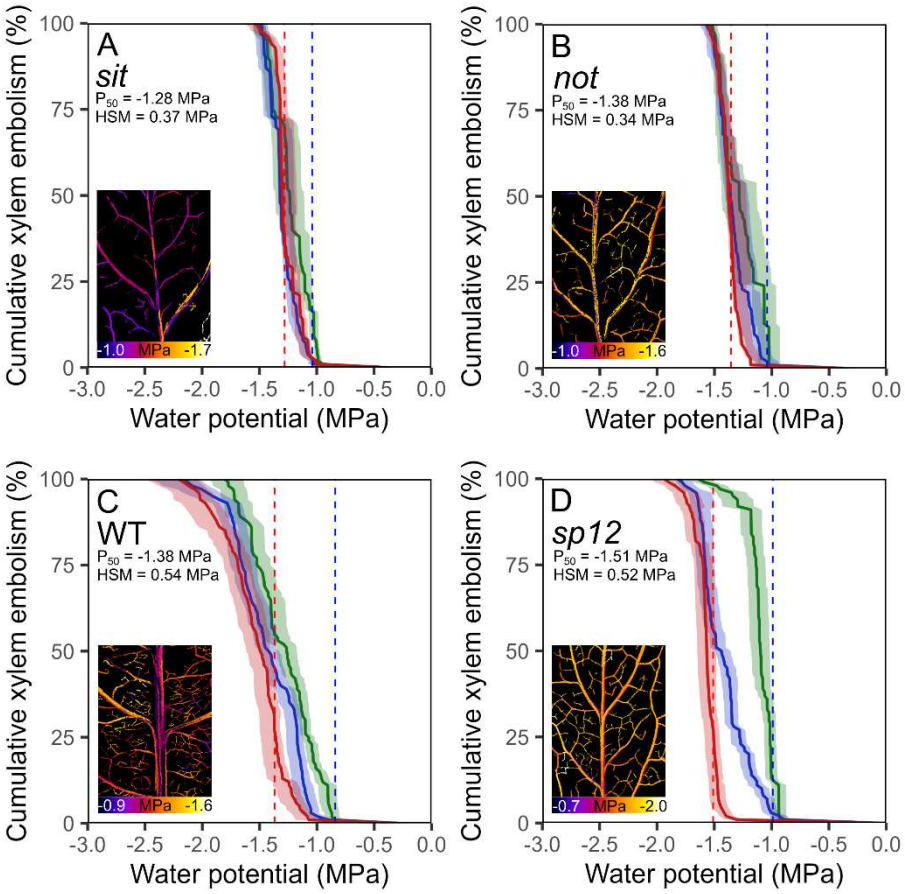

Figure 2. Optical vulnerability curves obtained from leaves of four tomato genotypes differing in their ability to accumulate foliar ABA: *sitiens (sit)* and *notabilis (not)* are ABA biosynthetic mutants, WT is wild type cv. Ailsa Craig, and *sp12* is a transgenic line over-accumulating ABA. Midrib is represented by green lines, secondary veins by blue lines, and minor veins by red lines. Data are mean (highlighted lines) ± standard error (shadow) (n = 6). Blue dashed lines represent leaf turgor loss points and red dashed lines indicate the water potentials associated with 50% of cumulative xylem embolism for the whole leaf (P_{50}). The difference between these two parameters is the hydraulic safety margin (HSM).

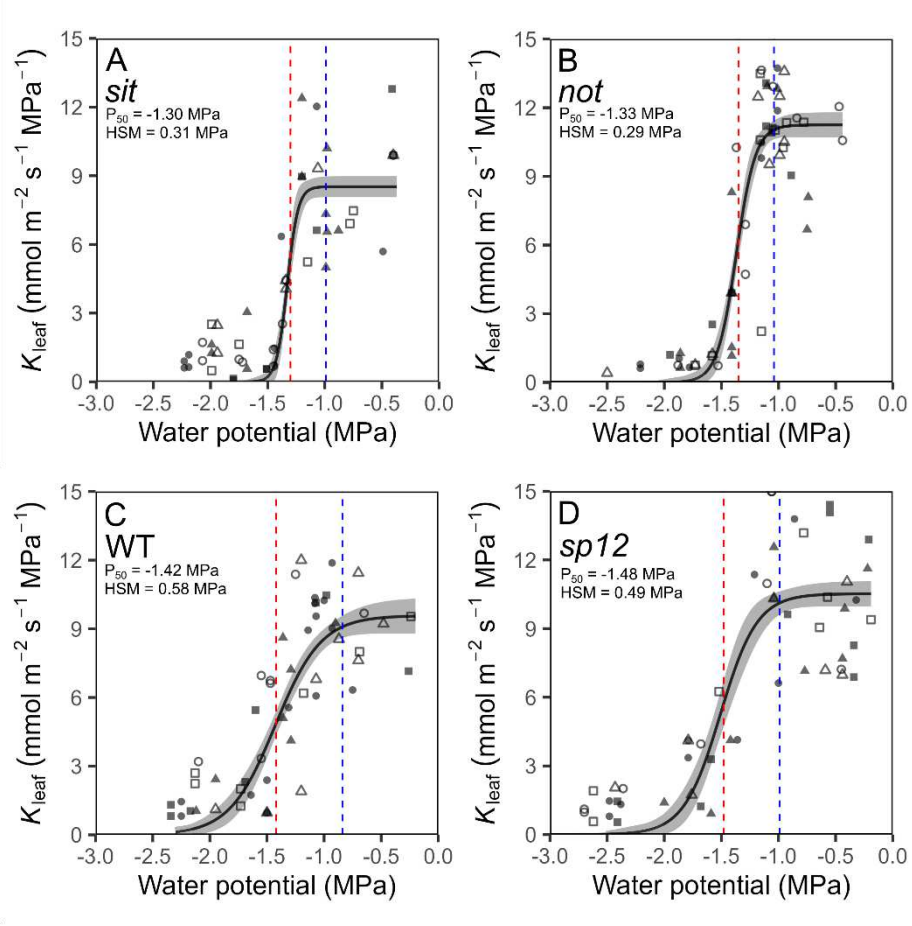

Figure 3. Decline in leaf hydraulic conductance (K_{leaf}) during leaf dehydration for four tomato genotypes differing in their ability to accumulate foliar ABA: *sitiens (sit)* and *notabilis (not)* are ABA biosynthetic mutants, WT is wild type cv. Ailsa Craig, and *sp12* is a transgenic line over-accumulating ABA. Black continuous lines are the predicted values from the three-parameter sigmoidal equation performed using all data and shadows represent standard errors. Different symbols indicate individual plants (n = 6). Blue dashed lines represent leaf turgor loss points and red dashed lines indicate the water potentials associated with 50% loss in K_{leaf} (P_{50}). The difference between these two parameters is the hydraulic safety margin (HSM).

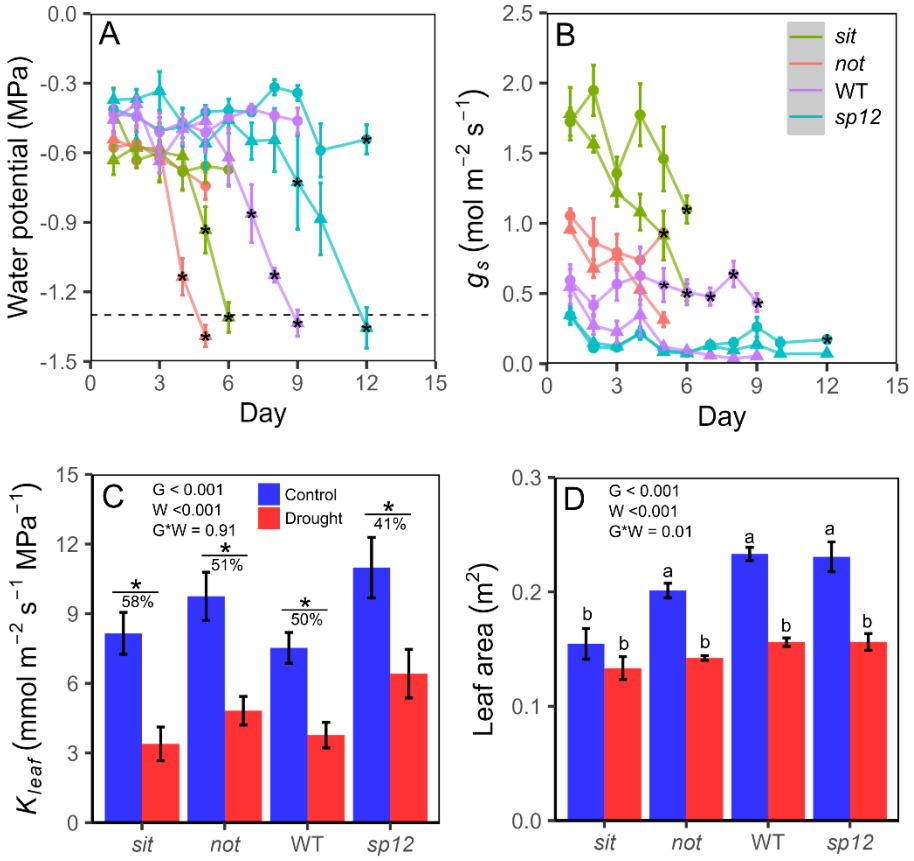

Figure 4. (A) Midday leaf water potential and (B) stomatal conductance (g_s) throughout a dry-down experiment of four tomato genotypes differing in their ability to accumulate foliar ABA: *sitiens (sit)* and *notabilis (not)* are ABA biosynthetic mutants, WT is wild type cv. Ailsa Craig, and *sp12* is a transgenic line over-accumulating ABA. Plants had water withheld after the first measurement and they were maintained under drought until the critical water potential of -1.30 MPa (black dashed line in A). Circles represent control plants and triangles, droughted plants. (C) Leaf hydraulic conductance (K_{leaf}) of control and droughted plants two days after irrigation was restored. (D) Plant leaf area at the end of the experiment. Data are mean ± standard error (n = 4). The two-way ANOVA results are shown (G=genotype; W=watering condition). Asterisks denote statistical differences (Tukey, p<0.05) for watering conditions (control versus drought) and letters allow comparison between treatments. See Fig S1 for representative images of plants during this experiment.

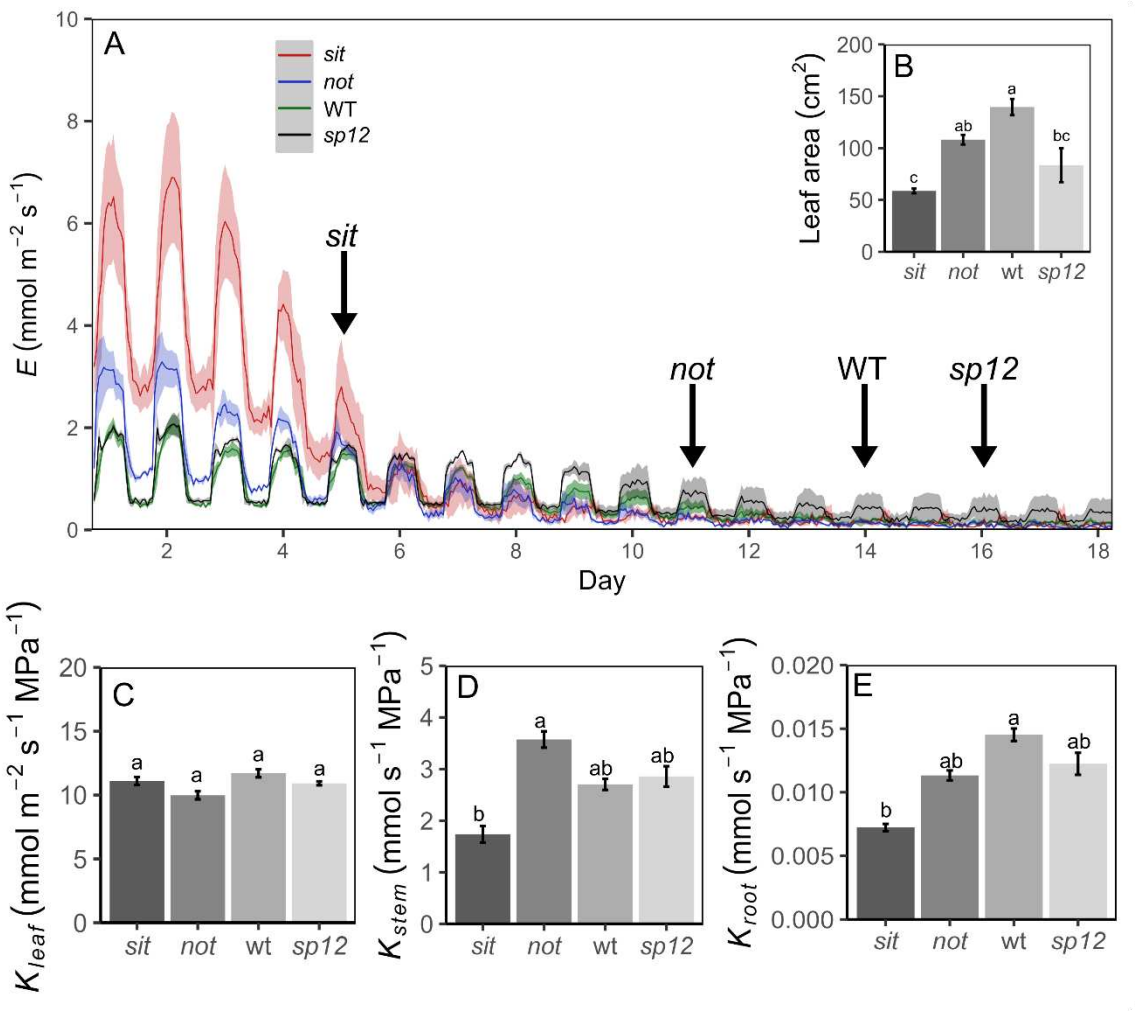

Figure 5. Dry-down experiment using seedlings of four tomato genotypes differing in their ability to accumulate foliar ABA: sitiens (sit) and notabilis (not) are ABA biosynthetic mutants, WT is wild type cv. Ailsa Craig, and sp12 is a transgenic line over-accumulating ABA. (A) Whole-plant transpiration rate throughout the drought days. Black arrows indicate the day at which plants from the four genotypes wilted. (B) Total leaf area per plant. (C) Leaf hydraulic conductance (K_{leaf}) normalized by leaf area. (D) Stem hydraulic conductance (K_{stem}). (E) Root hydraulic conductance (K_{root}). Shadows and error bars represent standard error (n = 4). Letters over the error bars denote results from statistical tests (Tukey, $p<0.05$) conducted between genotypes.

SUPPLEMENTARY DATA

Supplemental Table S1. A detailed description of the nutrient solution used for plant cultivation.

Stock solution		Formula Weight	kg m^{-3} of stock solution
A	$Mg(NO_3)_2 .6H_2O$	256.41	26
	$Ca(NO_3)_2 .4H_2O$	236.15	64
	Sequestrene 330 Fe 10% Fe		10
B	KNO_3	101.11	40.44
	NH_4NO_3	80.04	16
	KH_2PO_4	136.09	4.8
	K_2HPO_4	174.18	5.6
	K_2SO_4	174.27	6
	Na_2SO_4	142.04	6.8
	H_3BO_3	61.83	0.28
	$MoO_3.2H_2O$	179.97	0.002
	$ZnSO_4.7H_2O$	287.54	0.011
	$MnCl_2.4H_2O$	197.9	0.0816
	$CuSO_4.5H_2O$	249.7	0.004
	$CoCl_2.6H_2O$	237.9	0.00024

Supplemental Table S2. Water potential inducing 50% (P_{50}) embolism across leaf vein orders (midrib, secondary and minority veins) of four tomato genotypes differing in their ability to accumulate foliar ABA: *sitiens (sit)* and *notabilis (not)* are ABA biosynthetic mutants, WT is wild type cv. Ailsa Craig, and *sp12* is a transgenic line over-accumulating ABA.

Trait	*sit*	*not*	WT	*sp12*	*p*-value (genotypes)
$P_{50\ midrib}$	-1.23 ± 0.13	-1.32 ± 0.13	-1.26 ± 0.09	-1.10 ± 0.08^{A}	0.137
$P_{50\ secondary\ veins}$	-1.32 ± 0.02	-1.32 ± 0.06	-1.42 ± 0.08	-1.44 ± 0.05^{B}	0.106
$P_{50\ minority\ veins}$	-1.30 ± 0.03	-1.36 ± 0.03	-1.49 ± 0.12	-1.57 ± 0.08^{B}	0.472
p-value (veins)	0.718	0.926	0.252	0.001	

Data are mean ± standard error (n = 6). Superscript capital letters denote results from statistical tests (Tukey, $p<0.05$) conducted between vein orders.

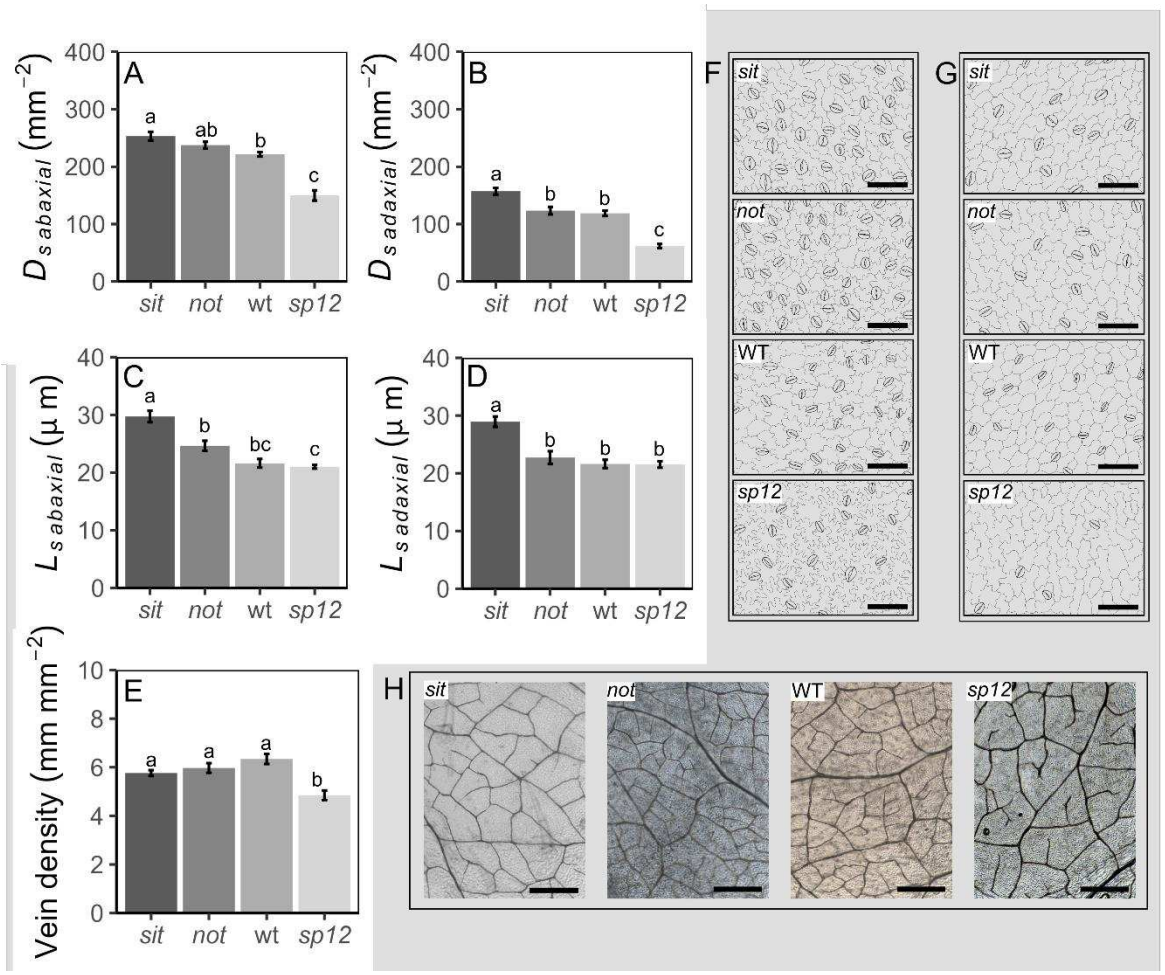

Supplemental Figure S1. (A, B) Stomatal density (D_s), (C, D) guard cell length (L_s), and (E) vein density of four tomato genotypes differing in their ability to accumulate foliar ABA: *sitiens (sit)* and *notabilis (not)* are ABA biosynthetic mutants, WT is wild type cv. Ailsa Craig, and *sp12* is a transgenic line over-accumulating ABA. (F-H) Representative images of stomatal distribution (scale bar: 100 µm) from the abaxial and adaxial epidermis, and leaf venation (scale bar: 500 µm) are depicted in F, G, and H, respectively. Data are mean ± standard error (n = 6). Letters over the error bars denote results from statistical tests (Tukey, p<0.05) conducted between genotypes.

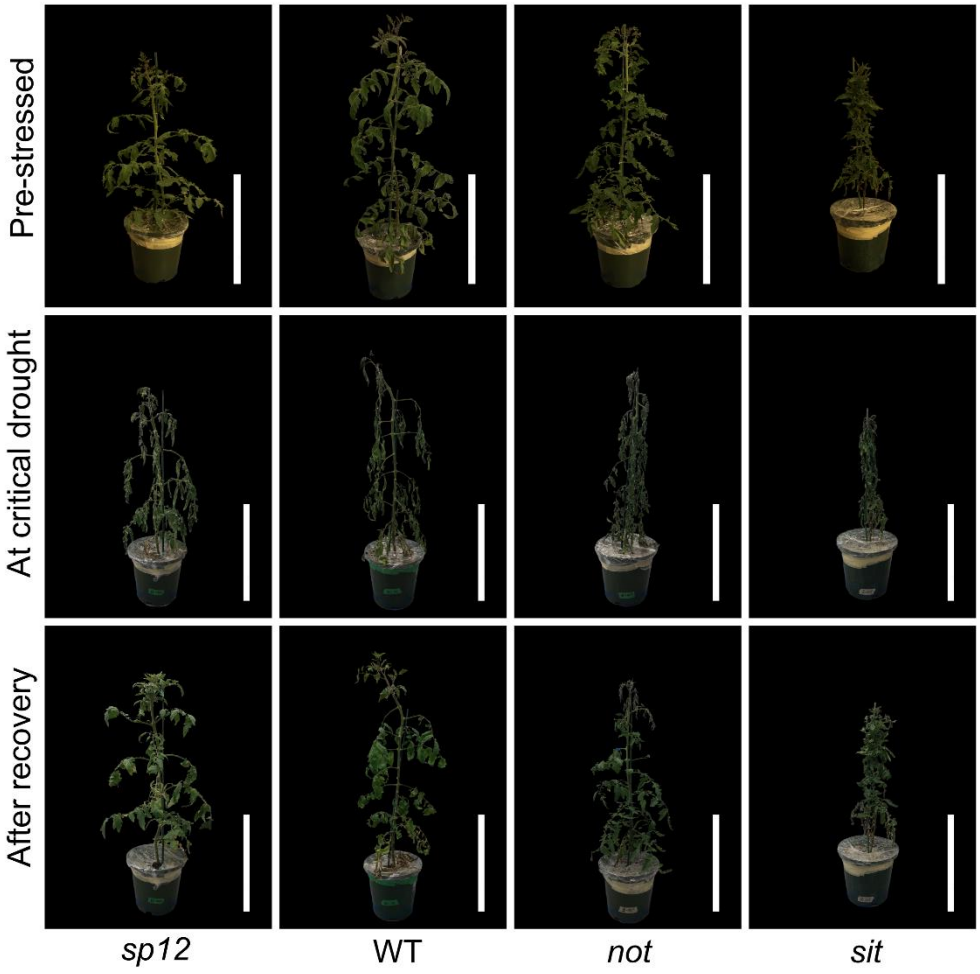

Supplemental Figure S2. Representative images of 60-day-old plants at the critical water potential of -1.30 MPa during the dry-down experiment and two days after irrigation was resumed (scale = 0.50 m). *Sitiens (sit)* and *notabilis (not)* are ABA biosynthetic mutants, WT is wild type cv. Ailsa Craig, and *sp12* is a transgenic line over-accumulating ABA.

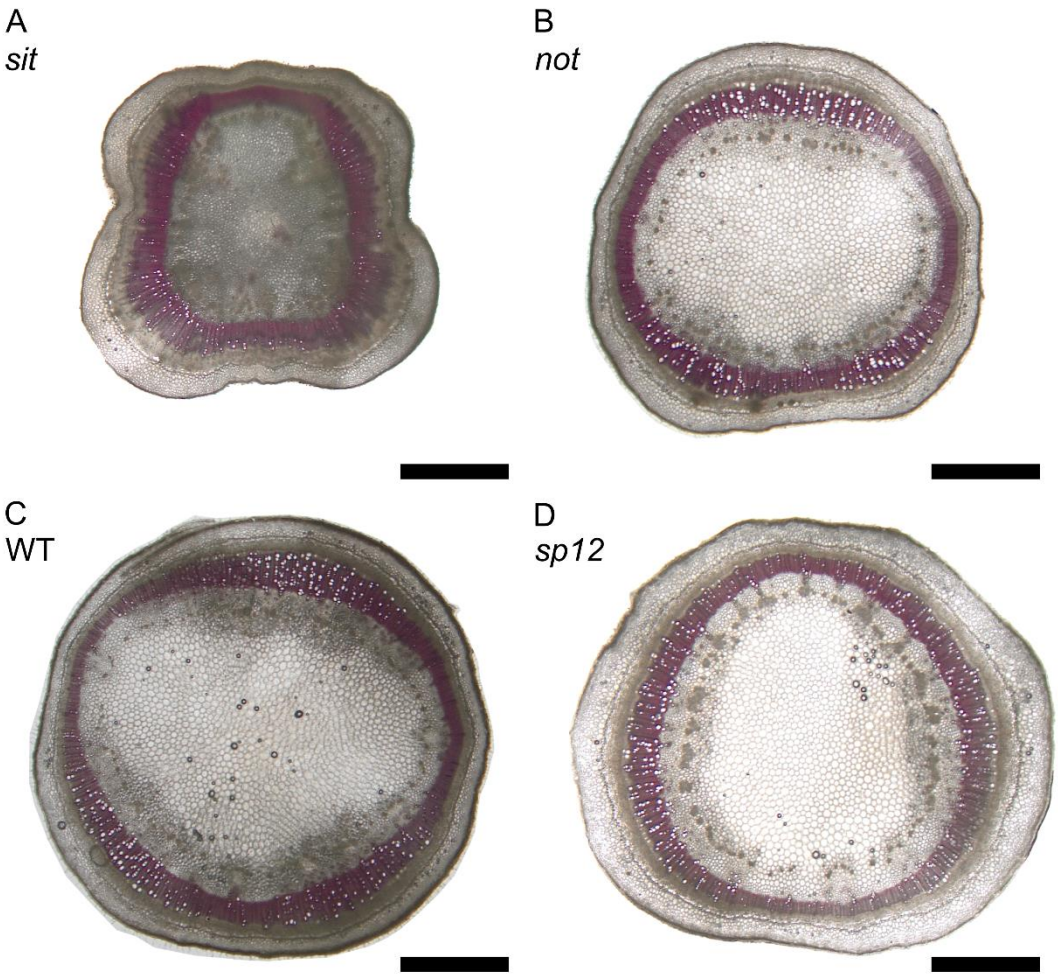

Supplemental Figure S3. Free-hand cross-sections of stems of 60-day-old tomato plants. Sections were stained with phloroglucinol, which stains lignin in red so that the xylem area can be easily recognized. Images are from four genotypes differing in their ability to accumulate foliar ABA: *sitiens (sit)* and *notabilis (not)* are ABA biosynthetic mutants, WT is wild type cv. Ailsa Craig, and *sp12* is a transgenic line over-accumulating ABA. Scale bars: 250 µm.

CHAPTER 2

Secondary growth increases embolism resistance in herbaceous plants

Eduardo J. Haverroth, Ian M. Rimer, Leonardo A. Oliveira, Leydson G. A. de Lima, Igor Cesarino, Samuel C. V. Martins, Scott A. M. McAdam, Amanda A. Cardoso

ABSTRACT

The stems of some herbaceous species can undergo basal secondary growth, leading to a continuum in the degree of woodiness along the stem. Whether the formation of secondary growth increases the embolism resistance of stems within herbaceous species is not yet known. We simultaneously assessed the embolism resistance of leaves and the basal and upper stems within the same individuals of two divergent herbaceous species that undergo secondary growth in mature stems, *Solanum lycopersicum* and *Senecio minimus.* We also examined whether differences in embolism resistance in the two stem portions were associated with alterations in anatomy and lignin content. The basal stem region with advanced secondary growth was more resistant to embolism, which resulted in vulnerability segmentation between the basal stem and the rest of the vegetative shoot. In addition to increased woodiness, greater embolism resistance in the basal stems occurred alongside decreases in the pith-to-xylem area, increases in the proportion of secondary xylem conduits, and increases in lignin content. Secondary growth in the basal stem of herbaceous plants might have evolved to increase survival through a phenologically-late drought or ensure structural support and continual water transport to a large upper canopy of leaves, flowers, and fruits.

INTRODUCTION

Water is transported through the stem from the soil to the evaporating surfaces in the leaf. This upward water movement against gravity is driven by a water potential gradient in the xylem conduits (Dixon & Joly 1895). During drought, the formation of embolism creates a lethal resistance to the water flow through xylem conduits. Embolism forms when increasingly negative pressure in the xylem occurs above a threshold that results in the movement of gas across pit membranes (Tyree & Sperry 1989; Kaack *et al.* 2021; Avila *et al.* 2022). As drought progresses, the spread of embolism throughout the xylem network results in tissue damage and ultimately mortality of the plant (Urli *et al.* 2013; Hammond *et al.* 2019; Cardoso *et al.* 2020; Brodribb *et al.* 2021).

Critical levels of embolism in the stem are directly associated with drought-induced mortality (Brodribb & Cochard 2009; Urli *et al.* 2013; Hammond *et al.* 2019) such that increased resistance to stem embolism represents an important drought tolerance mechanism that has evolved multiple times in land plants (McAdam & Cardoso 2019). Resistant xylem in stems may or may not be accompanied by similarly resistant xylem in leaves (Cardoso *et al.* 2022; Wilkening, Skelton, Feng, Dawson & Thompson 2023) – the latter being termed vulnerability segmentation. When leaves are less resistant to embolism than stems, they are the first organs to embolize during drought, acting as “hydraulic fuses” that break the soil-plant-atmosphere continuum before embolism spreads to stems – i.e. the critical organ defining plant mortality (Wolfe, Sperry & Kursar 2016; Wilkening *et al.* 2023). This drought tolerance mechanism has been demonstrated in several woody angiosperm and conifer species (Alder, Sperry & Pockman 1996; Sperry & Ikeda 1997; Choat, Lahr, Melcher, Zwieniecki & Holbrook 2005; Rodriguez-Dominguez *et al.* 2018; Skelton *et al.* 2019; Avila *et al.* 2021) but also not found in some species (Bouche *et al.* 2016; Klepsch *et al.* 2018; Li *et al.* 2020; Smith-Martin, Skelton, Johnson, Lucani & Brodribb 2020). In the case of herbaceous species, vulnerability segmentation between stems and leaves has been ruled out in two-month-old *Solanum lycopersicum* plants (Skelton et al., 2017) but found in three-month old plants of the same genotype (Harrison Day, Carins-Murphy & Brodribb 2022).

Research efforts have long focused on exploring the structural traits associated with increased stem xylem resistance to embolism (Lens *et al.* 2011, 2022; Levionnois

et al. 2021; Kaack *et al.* 2021; Johnson & Brodribb 2023). These studies have identified several key variables that are associated with increased stem resistance, including narrow xylem conduits with thicker cell walls, thicker pit membranes in interconduit pits, scattered distribution of xylem conduits, lower pith-to-xylem area, and a higher degree of woodiness. Most of these studies have only assessed woody species, with limited hypotheses tested about the anatomical drivers of embolism resistance in the stems of herbaceous species (Lens *et al.*, 2011, 2022).

Recent studies assessing the embolism resistance in the stems of herbaceous eudicot species have found that a greater embolism resistance is linked to increased woodiness in species that form wood – i.e., “woody herbs” or species that have evolved secondary woodiness on islands compared to the most recent herbaceous sister groups (Tixier *et al.* 2013; Lens *et al.* 2016; Dória *et al.* 2018, 2019; Thonglim *et al.* 2021). In these studies, the degree of stem woodiness is described as the proportion of lignified area per total stem area (i.e., primary xylem, secondary xylem, and fibers). Given that the secondary xylem is produced later than the primary xylem and only after the onset of secondary growth in stems, an increased stem woodiness can be directly associated with a higher proportion of secondary xylem conduits, exhibiting higher air-seeding thresholds compared with primary xylem conduits (Choat *et al.* 2005; Brodersen *et al.* 2013). Finally, in herbaceous species, the stem resistance to embolism seems to be less dependent on vessel diameter than in woody species, while the linkage between embolism resistance and intervessel pit membrane thickness remains ambiguous when assessed across species (Lens et al., 2016; Dória et al., 2019). In a study assessing the link between stem woodiness and embolism resistance in a herbaceous species, Thonglim et al. (2021), found that the more ‘woody’ mutant of Arabidopsis *soc1*, which was significantly more resistant than the wild type (Col-0) and that this increased resistance occurred along with thicker pit membranes.

The few studies assessing variations in stem embolism resistance in herbaceous plants compare either different species, different genotypes, or different individuals of the same species/genotype growing under different conditions (Lens et al., 2016; Cardoso et al., 2018 Dória et al., 2019). Few attempts have been made to assess variation in stem embolism resistance within the same individual. In some species of herb, secondary growth can occur especially at the base of the stems but not extending into the upper stem (Kidner *et al.* 2015). This form of growth makes these species the perfect model system to investigate a potential association between

woodiness and embolism resistance within individuals. In this study, we selected two herbaceous species that exhibit secondary growth in basal stems to assess whether increased woodiness at the base of the stem increases embolism resistance in that tissue. The species were: *Solanum lycopersicum* L. (Solanaceae) (Thompson & Heimsch 1964) and *Senecio minimus* Poir. (Asteraceae) (Wapstra et al., 2008). The anatomy of the stem portions and lignin contents were examined to investigate key structural and biochemical determinants associated with increased woodiness that might correlate with variation in stem embolism resistance in herbaceous species.

MATERIAL AND METHODS

Plant material

Plants of *Solanum* and *Senecio* were cultivated under controlled conditions in Raleigh, North Carolina (USA) and West Lafayette, Indiana (USA), respectively (Figure 1). Plants of *Solanum lycopersicum* cv. “Moneymaker” were cultivated from seeds in 6-L plastic pots containing a mixture of 33% Sun Gro Propagation Growing Mix (Canadian Sphagnum peat moss 50-65%, vermiculite, dolomitic lime, 0.0001% Silicon dioxide) and 66% pea gravel. Daily irrigation was performed to field capacity using nutrient solution (Supplementary Table S1). Plants were maintained in walk-in growth chambers and conditions were set to 18-h photoperiod with photosynthetic photon flux density (PPFD) of c. 600 µmol m^{-2} s^{-1}, and day:night temperature cycles of 26:22°C. At the onset of experiments, *Solanum* plants were five months old.

Plants of *Senecio minimus* [College Road population (McAdam, Brodribb, Ross & Jordan 2011)] were cultivated from seeds in 5-L pots containing commercial potting mix and were maintained under greenhouse conditions. Plants were watered daily and received weekly applications of liquid fertilizer (Miracle-Gro, Scotts Company LLC, OH, USA). Conditions in the greenhouse were 12-h photoperiod with maximum PPFD of c. 1500 µmol m^{-2} s^{-1}, and day:night temperatures of 28:22°C. At the onset of experiments, *Senecio* plants were approximately seven months old.

Optical vulnerability curves

Vulnerability curves of leaves and stems were constructed using the optical vulnerability method (Brodribb *et al.* 2016a). Plants were brought to the laboratory, removed from pots, and had their roots carefully washed. Plants were maintained overnight with their roots under water with aeration systems to ensure that observations started on fully-hydrated individuals. The next morning, leaves (the last fully expanded), the upper stems (<10 cm from the shoot tip), and the basal (<10 cm above the collar) stems from the same plant were used to construct vulnerability curves for each species (n = 5 plants for *Solanum* and n = 3 plants for *Senecio*).

The xylem of stems was carefully exposed using a razor blade or fingernail and covered with Tensive conductive adhesive gel and a cover slip. Stereomicroscopes were used for imaging the stem xylem of *Solanum* (LCD Digital Microscope, New York Microscope Company, NY, USA) and *Senecio* (AmScope with mounted AmScope digital camera MU1603, CA, USA). Reflected light was used for imaging stems of both species. The newest most fully expanded leaves of *Solanum* were imaged using Cavicams (cavicam.co) and in *Senecio* were imaged using the same stereomicroscopes for the stems. Transmitted light was used for imaging leaves of both species. Images of stems and leaves were taken every 180 s (for *Solanum*) or 300 s (for *Senecio*) as plants dehydrated under dark conditions. To ensure that all embolism events were captured, images were taken for at least 24 hours after the last embolism event was detected.

Embolism quantification was performed by subtracting subsequent images to reveal light transmission changes associated with xylem embolism (http://www.opensourceov.org) (Cardoso *et al.* 2022). Embolized pixels were expressed as a percentage of the total embolized pixel area. To construct the vulnerability curve, each embolism event was associated with the plant water potential (Ψ_w) at the moment that the image was taken. The Ψ_w was periodically measured (every 10-30 min) using a stem psychrometer (ICT, Armidale, Australia) for both species. Mean and standard errors for vulnerability curves were determined for every 1% of embolized xylem area and plotted as per (Cardoso *et al.* 2022). The Ψ_w at 12%, 50%, and 88% cumulative embolism (P_{12}, P_{50}, and P_{88}) were obtained for each curve. The time for the upper stem to embolize relative to the basal stem was obtained by dividing the time for the upper stem to reach P_{12}, P_{50}, and P_{88} by the time for the basal stem to reach the same embolism levels.

Stem anatomy

For both species, portions of the upper and basal stems similar to those used for constructing vulnerability curves were sampled for anatomical measurements. Samples were fixed in FAA70 for 48 h, stored in 70% ethanol (Johansen, 1940), dehydrated in a graded ethanol series, and embedded in HistoResin (HistoResin, Leica Microsystems, Heidelberg, Germany). Transverse sections of 10 µm were obtained with a rotary microtome (HistoCore Biocut, Leica Microsystems Inc., IL, USA), stained with toluidine blue, and mounted in Permount Mounting Medium (Permount®, Thermo Fisher Scientific Inc., MA, USA).

For each sample, one field of view (FOV) was taken using a digital camera (DP28, Olympus Optical, Tokyo, Japan) mounted on a stereo microscope (ZMS800, Nikon, Japan). From these images, we measured the area of the stem (A_{stem}), the xylem (A_{xylem}), and the pith (A_{pith}). The pith-to-xylem area ratio ($P_{pith:xylem}$) was calculated by dividing the A_{pith} by the A_{xylem}. Images were also taken using a digital camera (DP28, Olympus Optical, Tokyo, Japan) mounted on a light microscope (BX53, Olympus Optical, Tokyo, Japan). Three FOVs at 4x magnification were taken for each sample to estimate the proportion of secondary xylem vessels as a proportion to total xylem vessels ($P_{SecXylem}$) as well as the xylem cell wall thickness (t) and lumen breadth (b) ratio $[(t/b)^3]$ of all xylem vessels (including primary and secondary). The t was calculated as the average of four samples of xylem cell wall thickness of each vessel, and b was calculated as the average of the maximum and minimum diameters of each lumen. Last, five additional FOVs at 10x magnification were taken for each sample using a digital camera to obtain the vessel diameter (D_h). The vessel diameter (D_v) was calculated using the following equation, after measuring the longest (a) and shortest (b) internal diameters of all vessels imaged from each sample:

$$D_v = \sqrt{\frac{2a^1b^2}{a^2+b^2}} \quad (1)$$

The D_h was then calculated as (Sperry & Ikeda 1997):

$$D_h = \frac{\sum Dv^5}{\sum Dv^4} \quad (2)$$

Lignin analyses

To visualize lignin in the stem tissues, we prepared hand-cut transverse sections from fresh samples of the upper and basal stems. The sections were stained for 5 min with a solution containing phloroglucinol–HCl (1:2) [2% (w:v) phloroglucinol in 95% alcohol and 5 M hydrochloric acid] (adapted from Johansen, 1940). Representative images were taken using the same digital camera and light microscope described above.

For both plant species, the upper and basal stems similar to those used for constructing vulnerability curves were used to quantify lignin content. Samples were dried and ball-milled to a fine powder using the TissueLyser (QUIAGEN, Germany). Dry plant material was successively extracted with water (98°C), ethanol (76°C), ethanol:chloroform 1:1 v/v (59°C), and acetone (54°C), for 15 min at 750 rpm each. The resulting purified cell wall residue (CWR) was dried at 60°C overnight and used for lignin quantification using the acetyl bromide method (Fukushima & Kerley 2011). The absorbance at 280 nm was measured using a NanoDrop® ND-1000 spectrophotometer (ThermoFisher, USA). Lignin contents were calculated using the Bouguer-Lambert-Beer law:

$$C = \frac{A}{(\varepsilon * \mathrm{l}) * 10} \quad (3)$$

where C = total amount of lignin in mg, A = absorbance at 280 nm, ε = extinction coefficient (23.0772 g^{-1} L cm^{-1} (Fukushima & Kerley 2011)), l = path length of 0.1 cm, and 10 = dilution factor. The total amount of lignin was divided by the amount of CWR and multiplied by 100 to provide lignin concentration.

Statistical analysis

Data were tested for normality using the Shapiro-Wilk test. One-way ANOVA followed by the Tukey post-hoc test was performed to test the differences in embolism resistance among leaves, apical stems, and basal stems. Student's *t*-test was applied to test differences in time for the upper stems to reach critical water potentials relative to the basal stems as well as anatomical differences between the upper and the basal stems. All statistical analyses and plots were performed using RStudio (version 4.3.0).

RESULTS

Basal stems were more resistant to embolism than upper stems and leaves

Significant vulnerability segmentation across the stem and between basal stems and leaves was observed for both species (Figure 2, Table 1). In both species, basal stems were more resistant to embolism than both the upper stems and leaves (Figure 1, Table 1). Differences in embolism resistance between the upper and basal stems were observed in terms of P_{12}, P_{50}, and P_{88} (Table 1). For both species, the mean basal stem P_{50} was c. -0.93 MPa (-0.88 for *Solanum* and -0.99 for *Senecio*) higher than the mean upper stem P_{50}. Differences in embolism resistance were also observed in terms of the times to reach the P_{12}, P_{50}, and P_{88} (Table 2). The upper stem of both species reached 12, 50, and 88% levels of embolism in between 51-63% of the time taken to reach similar embolism thresholds in the basal stem.

Leaves of both species were similarly resistant to embolism to the corresponding upper stems but less resistant to embolism than the basal stems (Figure 1, Table 1). The differences between the mean basal stem P_{50} and leaf P_{50} were -1.10 MPa for *Solanum* and -1.30 for *Senecio*.

Major structural and biochemical alterations occur across stems

Basal stems of both species were consistently wider than the upper stem (Figure 1; A_{stem} in Table 3). Differences in woodiness were visible in both species as the basal stems were considerably more rigid and darker than the upper stems. These differences were also observed at the anatomical level (Figure 3).

In the upper stems of *Solanum*, the transition from primary to secondary growth had already been initiated (Figure 3). This transition manifested as a continuous vascular cylinder composed of secondary xylem surrounding the pith. Secondary xylem vessels represented nearly 60% of the total xylem vessels but primary xylem vessels were still intact and immersed in the outermost part of the pith. The basal stem of *Solanum* was at a later stage of secondary growth. The stem shape had transitioned from circular to triangular as the secondary xylem expanded toward three opposing directions. Most secondary xylem vessels were confined to these three distinct vertices, but vessels occurred throughout the whole vascular cylinder. The secondary

xylem had expanded considerably at this stage so that over 90% of the total xylem vessels consisted of secondary xylem vessels (Figure 3). Also, the A_{xylem} of the basal stem was over 10 times greater than that of the upper stem (Table 3). In contrast, the A_{pith} of the basal stem was similar to that of the upper stem. Thus, $P_{pith:xylem}$ was substantially lower in the basal stem than in the upper stem (Figure 3). Xylem vessels were wider (D_h was 25% higher) in the basal stem compared to the upper stem but the $(t/b)^3$ was similar between the two stem portions (Table 3).

For *Senecio*, the basal regions of the stem exhibited advanced secondary growth, while the upper regions had only begun to initiate a secondary cambium, having not yet fully formed a continuous vascular cylinder composed of secondary xylem (Figure 3). The basal stem was at a later stage of secondary growth, with a much larger A_{xylem} and nearly 90% of the secondary xylem out of the total xylem vessels (Table 3; Figure 3). Secondary xylem vessels were grouped into radial groups separated by several layers of ray parenchyma. Primary xylem vessels were still visible in the outermost part of the pith. Given the large increases in the xylem area, the $P_{pith:xylem}$ was much lower in the basal stem (0.18) than in the upper stem (2.62) (Figure 3). Xylem vessels were 80% larger at the basal stem compared to the upper stem. The $(t/b)^3$ was similar between the two stem portions (Table 3).

Lignin content was highest in the basal stem

No differences in CWR content were observed between the basal and upper portions of the stems for both species (Figure 4). However, the lignin content per CWR was significantly higher in the basal stem when compared to the upper stem, and such differences were more prominent for *Senecio*.

DISCUSSION

Vulnerability segmentation occurs within individual stems of woody herbaceous

Vulnerability segmentation has long been demonstrated across the different vegetative (summarized in Cardoso et al., 2022 and Wilkening et al., 2023) and reproductive (Zhang & Brodribb 2017; Bourbia, Carins-Murphy, Gracie & Brodribb 2020) organs of a species. Vulnerability segmentation within organs, however, has

only recently been demonstrated using the optical vulnerability method. Within leaves, for instance, higher vein orders are more resistant than lower vein orders (Brodribb *et al.* 2016b). Within the root system, larger roots close to the root collar are less resistant to embolism than smaller, peripheral roots (Harrison Day et al., 2023). In this study, we show that vulnerability segmentation occurs within individual stems of woody herbaceous species, in which the basal stem portion is more resistant to embolism than the upper stem portion.

For the two woody herbs, *Solanum* and *Senecio,* leaves and the upper stems were similarly resistant to embolism. However, both were less resistant than the basal region of the stems. The embolism resistance of the leaves as well as the basal and upper portions of the stem were assessed in the same plants, and the same pattern of embolism resistance across these organs/regions was observed in all plants analyzed. Therefore, we can consider that older plants of woody herbs exhibiting secondary growth in stems are likely to display vulnerability segmentation between leaves and the stem. Lack of vulnerability segmentation between leaves and stems has been observed for young plants (two months old) of *Solanum* (Skelton *et al.* 2017), but not for older plants (three months old) of the same species (Harrison Day *et al.* 2022). In light of our findings, we can only assume that such contrasting results between the two studies arose from the lack of secondary growth in the stems of the two-month-old plants of *Solanum* and the presence of secondary growth in the three-month-old plants.

During drought, xylem embolism in the stem above critical thresholds can lead to dehydration and mortality of all stem cells, including those of the meristematic tissues, which is critical for plant recovery from drought (Mantova, Herbette, Cochard & Torres-Ruiz 2022). Greater embolism resistance in the woody portions of the stem might represent a drought tolerance mechanism by which plants prevent dehydration and mortality of meristematic cells, allowing plants to better recover after drought. For that to occur, however, roots must also be able to withstand similarly high xylem tensions. Given that roots can also undergo secondary growth, both the basal stems and the root collars might exhibit greater embolism resistance thus leading to an overall higher plant tolerance to drought.

The onset of secondary growth in the basal stems of herbaceous plants occurs during the early reproductive phase, which means that it is possible that the production of lignified wood simply evolved to provide structural support to the flowers and fruits and to ensure hydraulic supply to an increased canopy area. The production of new

xylem, might represent a beneficial trait increasing the xylem conductive area to supply water to the new reproductive organs, especially to flowers that have been recently demonstrated to lose substantially more water through transpiration than leaves (Roddy et al., 2023). Increases in stem resistance to embolism in this case may simply be a consequence of increased degree of woodiness for reasons other than embolism resistance, nonetheless contributing to safely maintain the water supply to leaves and reproductive organs during drought (Harrison Day *et al.* 2022).

Increased stem woodiness associates with structural and biochemical alterations that enhance embolism resistance

The association between the degree of woodiness and embolism resistance within individual stems of *Solanum* and *Senecio* supports recent findings describing increases in stem resistance throughout the development of *Solanum* plants (Lamarque *et al.* 2020). A closer observation of the stem sections presented in this study demonstrates that young plants of tomato (50 days old) had just started transitioning from primary to secondary growth, while older plants (120 days old) were at a later stage of secondary growth. These findings highlight the importance of standardizing the developmental stage as well as the region of the stem to be selected to construct vulnerability curves so that reliable comparisons within and between herbaceous species can be performed.

Amongst the anatomical traits evaluated in the present study, the $P_{pith:xylem}$ and $P_{SecXylem}$ are ideal candidates to mechanistically explain the greater embolism resistance in the woody basal stem. In this study, an increase in xylem resistance was accompanied by a lower $P_{pith:xylem}$ in both species, similar to what was found for branches of a tree conifer (*Callitris rhomboidea*) (Johnson & Brodribb, 2023). In the later study, the lower $P_{pith:xylem}$ in more resistant branchlets was a consequence of a lower A_{pith} and a similar A_{xylem}. In our study, however, the lower $P_{pith:xylem}$ was a consequence of both a lower A_{pith} and a higher A_{xylem} in *Senecio*, and of a similar A_{pith} and a higher A_{xylem} in *Solanum.* The pith cells have long been suggested to act as a reservoir of gas for embolism seeding. First, the pith cells contain far more air than the surrounding xylem conduits (Holbrook, Ahrens, Burns & Zwieniecki 2001; Choat *et al.* 2010). Second, the first embolisms formed in the stems occur in xylem conduits located directly adjacent to the pith (Brodersen *et al.* 2013; Cochard, Delzon & Badel 2015;

Choat, Brodersen & McElrone 2015; Choat *et al.* 2016). Embolism would then spread from the central regions of the stem (where the pith is located) towards the outermost parts of the A_{xylem} in a radial pattern (Brodersen *et al.* 2013). If these theories hold true, not only does a lower A_{pith} represent a smaller gas reservoir but also a larger A_{xylem} represents a longer path for the spread of embolism, mechanistically explaining how a lower $P_{pith:xylem}$ can result in higher embolism resistance.

An increased woodiness in the base of stems was also accompanied by a higher $P_{SecXylem}$ for the two woody herbs evaluated in this study. Secondary xylem conduits have been demonstrated to be more resistant to embolism than those of the primary xylem in several species, including woody angiosperms (Choat *et al.* 2005; Venturas *et al.* 2019) and gymnosperms (Miller & Johnson 2017). Through micro-CT analyses, embolism was observed to form first in primary xylem conduits (Brodersen *et al.*, 2013; Choat et al., 2015), supporting the idea that primary xylem conduits are less resistant to embolism than secondary xylem conduits. Such difference in xylem resistance between conduits of the primary and secondary xylem is seemly associated with structural differences in their secondary wall. Vessels of the secondary xylem exhibit pitted secondary walls that provide stronger support to the pit membrane (primary cell wall) than the helical, annular, or scalariform secondary walls of the primary xylem vessels (Esau 1977). Consequently, vessels of the primary xylem have a greater area of pit membrane exposed, yielding them more susceptible to stretching and deflection (Choat *et al.* 2005), and thus to embolism formation. Therefore, a higher proportion of secondary xylem conduits in the woody base of herbs can also mechanistically explain the higher embolism resistance in this region. Further investigations are necessary to confirm whether pit membranes differ between conduits of the primary and secondary xylem, which can further explain the contrasting embolism resistance between the different regions of stems of woody herbaceous.

Previous studies on woody herbs that demonstrate the importance of secondary growth to increases in stem embolism resistance quantified the proportion of lignified area per total stem area to represent the degree of stem woodiness (Tixier *et al.* 2013; Lens *et al.* 2016; Dória *et al.* 2018, 2019). Such lignified areas included the primary and the secondary xylem as well as fibers. Given that the production of primary xylem is completed by the onset of secondary growth, we can infer that stems with higher lignified area per total stem area would also have a higher $P_{SecXylem}$ (*Lens et al., 2016; Doria et al., 2019*), similarly to what we found in the present study.

In addition to the higher $P_{SecXylem}$ in the basal stems, we also found that this portion displayed a higher lignin content per CWR. This increased deposition of lignin might have directly translated into a higher embolism resistance, especially if this occurred in the pit membranes of the xylem conduits. The presence of lignin in the pit membranes can potentially improve the mechanical strength of the pit membrane, thus reducing the susceptibility to stretching and deflection (Pereira, Domingues-Junior, Jansen, Choat & Mazzafera 2018). Lignin has been detected in the pit membrane of woody species (Fromm et al., 2003; Schmitz et al., 2008; Herbette et al., 2015), but has not been described in herbs. Therefore, further studies are necessary to investigate whether the presence of lignin in pit membranes plays a role in embolism resistance in herbs, explaining the increased resistance in the woody base of stems.

Finally, neither a smaller xylem vessel diameter nor a higher $(t/b)^3$ were associated with the higher embolism resistance found at the basal stems for *Solanum* and *Senecio*. In fact, both species displayed increases in tip-to-base widening of xylem vessels in parallel to increases in xylem resistance to embolism. Even though several studies have demonstrated an association between vessel diameter and resistance to embolism across angiosperms, a mechanistic explanation for such an association was never found (Lens *et al.* 2022). Additionally, several studies that do not find a link between smaller vessels and higher embolism resistance indicate that this assumption requires a critical re-evaluation, especially within single species and individuals (Lens *et al.* 2022).

CONCLUSION

An increased degree of woodiness in the basal stems of herbaceous plants results in higher embolism resistance. Structural and biochemical alterations underlying the higher embolism resistance in the woody base of stems include a lower pith-to-xylem area, a higher proportion of secondary xylem conduits, and higher lignin content. Increases in embolism resistance in the basal stem of herbaceous species likely increase the chances of survival through a phenologically-late drought. However, the production of lignified wood in the basal stem during the early reproductive stage might have simply evolved to improve the structural support of stems to hold erect a large upper canopy of leaves, flowers, and fruits.

Acknowledgments

This study was supported by the USDA National Institute of Food and Agriculture, Hatch Project 7003279 (AAC), and the National Science Foundation, Grant IOS-2140119 (SAMM).

REFERENCES

Alder N.N., Sperry J.S. & Pockman W.T. (1996) Root and stem xylem embolism, stomatal conductance, and leaf turgor in *Acer grandidentatum* populations along a soil moisture gradient. *Oecologia* **105**, 293–301.

Avila R.T., Cardoso A.A., Batz T.A., Kane C.N., DaMatta F.M. & McAdam S.A.M. (2021) Limited plasticity in embolism resistance in response to light in leaves and stems in species with considerable vulnerability segmentation. *Physiologia Plantarum* **172**, 2142–2152.

Avila R.T., Guan X., Kane C.N., Cardoso A.A., Batz T.A., DaMatta F.M., … McAdam S.A.M. (2022) Xylem embolism spread is largely prevented by interconduit pit membranes until the majority of conduits are gas-filled. *Plant Cell and Environment* **45**, 1204–1215.

Bouche P.S., Delzon S., Choat B., Badel E., Brodribb T.J., Burlett R., … Jansen S. (2016) Are needles of *Pinus pinaster* more vulnerable to xylem embolism than branches? New insights from X-ray computed tomography. *Plant Cell and Environment* **39**, 860–870.

Bourbia I., Carins-Murphy M.R., Gracie A. & Brodribb T.J. (2020) Xylem cavitation isolates leaky flowers during water stress in pyrethrum. *New Phytologist* **227**, 146–155.

Brodersen C.R., Mcelrone A.J., Choat B., Lee E.F., Shackel K.A. & Matthews M.A. (2013) In vivo visualizations of drought-induced embolism spread in *vitis vinifera*. *Plant Physiology* **161**, 1820–1829.

Brodribb T., Brodersen C.R., Carriqui M., Tonet V., Rodriguez Dominguez C. & McAdam S. (2021) Linking xylem network failure with leaf tissue death. *New Phytologist* **232**, 68–79.

Brodribb T.J., Bienaimé D. & Marmottant P. (2016a) Revealing catastrophic failure of leaf networks under stress. *Proceedings of the National Academy of Sciences of the United States of America* **113**, 4865–4869.

Brodribb T.J. & Cochard H. (2009) Hydraulic failure defines the recovery and point of death in water-stressed conifers. *Plant Physiology* **149**, 575–584.

Brodribb T.J., Skelton R.P., Mcadam S.A.M., Bienaimé D., Lucani C.J. & Marmottant P. (2016b) Visual quantification of embolism reveals leaf vulnerability to hydraulic failure. *New Phytologist* **209**, 1403–1409.

Cardoso A.A., Batz T.A. & McAdam S.A.M. (2020) Xylem embolism resistance determines leaf mortality during drought in *Persea americana*. *Plant Physiology* **182**, 547–554.

Cardoso A.A., Kane C.N., Rimer I.M. & McAdam S.A.M. (2022) Seeing is believing: what visualising bubbles in the xylem has revealed about plant hydraulic function. *Functional Plant Biology* **49**, 759–772.

Choat B., Badel E., Burlett R., Delzon S., Cochard H. & Jansen S. (2016) Noninvasive measurement of vulnerability to drought-induced embolism by X-Ray microtomography. *Plant Physiology* **170**, 273–282.

Choat B., Brodersen C.R. & McElrone A.J. (2015) Synchrotron X-ray microtomography of xylem embolism in *Sequoia sempervirens* saplings during cycles of drought and recovery. *New Phytologist* **205**, 1095–1105.

Choat B., Drayton W.M., Brodersen C., Matthews M.A., Shackel K.A., Wada H.I.R. & McElrone A.J. (2010) Measurement of vulnerability to water stress-induced cavitation in grapevine: A comparison of four techniques applied to a long-vesseled species. *Plant, Cell and Environment* **33**, 1502–1512.

Choat B., Lahr E.C., Melcher P.J., Zwieniecki M.A. & Holbrook N.M. (2005) The spatial pattern of air seeding thresholds in mature sugar maple trees. *Plant, Cell and Environment* **28**, 1082–1089.

Cochard H., Delzon S. & Badel E. (2015) X-ray microtomography (micro-CT): A reference technology for high-resolution quantification of xylem embolism in trees. *Plant, Cell and Environment* **38**, 201–206.

Dixon H.H. & Joly J. (1895) On the ascent of sap. *Philosophical Transactions of the Royal Society of London. (B.)* **186**, 563–576.

Dória L.C., Meijs C., Podadera D.S., del Arco M., Smets E., Delzon S. & Lens F. (2019) Embolism resistance in stems of herbaceous Brassicaceae and Asteraceae is linked to differences in woodiness and precipitation. *Annals of Botany* **124**, 1–14.

Dória L.C., Podadera D.S., Arco M., Chauvin T., Smets E., Delzon S. & Lens F. (2018) Insular woody daisies (*Argyranthemum*, Asteraceae) are more resistant to drought-induced hydraulic failure than their herbaceous relatives. *Functional Ecology* **32**, 1467–1478.

Esau K. (1977) *Anatomy of seed plants*, 2nd ed. John Wiley & Sons Ltd, New York.

Fromm J., Rockel B., Lautner S., Windeisen E. & Wanner G. (2003) Lignin distribution in wood cell walls determined by TEM and backscattered SEM techniques. *Journal of Structural Biology* **143**, 77–84.

Fukushima R.S. & Kerley M.S. (2011) Use of lignin extracted from different plant sources as standards in the spectrophotometric acetyl bromide lignin method. *Journal of Agricultural and Food Chemistry* **59**, 3505–3509.

Hammond W.M., Yu K., Wilson L.A., Will R.E., Anderegg W.R.L. & Adams H.D. (2019) Dead or dying? Quantifying the point of no return from hydraulic failure in drought-induced tree mortality. *New Phytologist* **223**, 1834–1843.

Harrison Day B.L., Carins-Murphy M.R. & Brodribb T.J. (2022) Reproductive water supply is prioritized during drought in tomato. *Plant Cell and Environment* **45**, 69–79.

Harrison Day B.L., Johnson K.M., Tonet V., Bourbia I., Blackman C. & Brodribb T.J. (2023) The root of the problem: diverse vulnerability to xylem cavitation found within the root system of wheat plants. *New Phytologist*.

Herbette S., Bouchet B., Brunel N., Bonnin E., Cochard H. & Guillon F. (2015) Immunolabelling of intervessel pits for polysaccharides and lignin helps in understanding their hydraulic properties in Populus tremula × alba. *Annals of Botany* **115**, 187–199.

Holbrook N.M., Ahrens E.T., Burns M.J. & Zwieniecki M.A. (2001) In vivo observation of cavitation and embolism repair using magnetic resonance imaging. *Plant Physiology* **126**, 27–31.

Johansen D.A. (1940) *Plant microtechnique*. McGraw-Hill, New York.

Johnson K.M. & Brodribb T.J. (2023) Evidence for a trade-off between growth rate and xylem cavitation resistance in *Callitris rhomboidea*. *Tree Physiology* **00**, 1–11.

Kaack L., Weber M., Isasa E., Karimi Z., Li S., Pereira L., … Jansen S. (2021) Pore constrictions in intervessel pit membranes provide a mechanistic explanation for xylem embolism resistance in angiosperms. *New Phytologist* **230**, 1829–1843.

Kidner C., Groover A., Thomas D.C., Emelianova K., Soliz-Gamboa C. & Lens F. (2015) First steps in studying the origins of secondary woodiness in Begonia (Begoniaceae): combining anatomy, phylogenetics, and stem transcriptomics. *Biological Journal of the Linnean Society* **117**, 121–138.

Klepsch M., Zhang Y., Kotowska M.M., Lamarque L.J., Nolf M., Schuldt B., … Jansen S. (2018) Is xylem of angiosperm leaves less resistant to embolism than branches? Insights from microCT, hydraulics, and anatomy. *Journal of Experimental Botany* **69**, 5611–5623.

Lamarque L.J., Delzon S., Toups H., Gravel A.I., Corso D., Badel E., … Gambetta G.A. (2020) Over-accumulation of abscisic acid in transgenic tomato plants increases the risk of hydraulic failure. *Plant Cell and Environment* **43**, 548–562.

Lens F., Gleason S.M., Bortolami G., Brodersen C., Delzon S. & Jansen S. (2022) Functional xylem characteristics associated with drought-induced embolism in angiosperms. *New Phytologist* **236**, 2019–2036.

Lens F., Picon-Cochard C., Delmas C.E.L., Signarbieux C., Buttler A., Cochard H., … Delzon S. (2016) Herbaceous angiosperms are not more vulnerable to drought-induced embolism than angiosperm trees. *Plant Physiology* **172**, 661–667.

Lens F., Sperry J.S., Christman M.A., Choat B., Rabaey D. & Jansen S. (2011) Testing hypotheses that link wood anatomy to cavitation resistance and hydraulic conductivity in the genus Acer. *New Phytologist* **190**, 709–723.

Levionnois S., Jansen S., Wandji R.T., Beauchêne J., Ziegler C., Coste S., … Heuret P. (2021) Linking drought-induced xylem embolism resistance to wood anatomical traits in Neotropical trees. *New Phytologist* **229**, 1453–1466.

Li X., Delzon S., Torres-Ruiz J., Badel E., Burlett R., Cochard H., … Ximeng Li westernsydneyeduau (2020) Lack of vulnerability segmentation in four angiosperm tree species: evidence from direct X-ray microtomography observation. *Annals of Forest Science* **77**.

Mantova M., Herbette S., Cochard H. & Torres-Ruiz J.M. (2022) Hydraulic failure and tree mortality: from correlation to causation. *Trends in Plant Science* **27**, 335–345.

McAdam S.A.M., Brodribb T.J., Ross J.J. & Jordan G.J. (2011) Augmentation of abscisic acid (ABA) levels by drought does not induce short-term stomatal sensitivity to CO_2 in two divergent conifer species. *Journal of Experimental Botany* **62**, 195–203.

McAdam S.A.M. & Cardoso A.A. (2019) The recurrent evolution of extremely resistant xylem. *Annals of Forest Science* **76**, 2–5.

Miller M.L. & Johnson D.M. (2017) Vascular development in very young conifer seedlings: Theoretical hydraulic capacities and potential resistance to embolism. *American Journal of Botany* **104**, 979–992.

Pereira L., Domingues-Junior A.P., Jansen S., Choat B. & Mazzafera P. (2018) Is embolism resistance in plant xylem associated with quantity and characteristics of lignin? *Trees* **32**, 349–358.

Rodriguez-Dominguez C.M., Carins Murphy M.R., Lucani C. & Brodribb T.J. (2018) Mapping xylem failure in disparate organs of whole plants reveals extreme resistance in olive roots. *New Phytologist* **218**, 1025–1035.

Schmitz N., Koch G., Schmitt U., Beeckman H. & Koedam N. (2008) Intervessel pit structure and histochemistry of two mangrove species as revealed by cellular UV microspectrophotometry and electron microscopy: Intraspecific variation and functional significance. *Microscopy and Microanalysis* **14**, 387–397.

Skelton R.P., Anderegg L.D.L., Papper P., Reich E., Dawson T.E., Kling M., … Ackerly D.D. (2019) No local adaptation in leaf or stem xylem vulnerability to embolism, but consistent vulnerability segmentation in a North American oak. *New Phytologist* **223**, 1296–1306.

Skelton R.P., Brodribb T.J. & Choat B. (2017) Casting light on xylem vulnerability in an herbaceous species reveals a lack of segmentation. *New Phytologist* **214**, 561–569.

Smith-Martin C.M., Skelton R.P., Johnson K.M., Lucani C. & Brodribb T.J. (2020) Lack of vulnerability segmentation among woody species in a diverse dry sclerophyll woodland community. *Functional Ecology* **34**, 777–787.

Sperry J.S. & Ikeda T. (1997) Xylem cavitation in roots and stems of Douglas-fir and white fir. *Tree Physiology* **17**, 275–280.

Thompson N.P. & Heimsch C. (1964) Stem anatomy and aspects of development in tomato. *American Journal of Botany* **51**, 7–19.

Thonglim A., Delzon S., Larter M., Karami O., Rahimi A., Offringa R., … Lens F. (2021) Intervessel pit membrane thickness best explains variation in embolism resistance amongst stems of *Arabidopsis thaliana* accessions. *Annals of Botany* **128**, 171–182.

Tixier A., Cochard H., Badel E., Dusotoit-Coucaud A., Jansen S. & Herbette S. (2013) Arabidopsis thaliana as a model species for xylem hydraulics: Does size matter? *Journal of Experimental Botany* **64**, 2295–2305.

Tyree M.T. & Sperry J.S. (1989) Vulnerability of xylem to cavitation and embolism. *Annual Review of Plant Physiology and Plant Molecular Biology* **40**, 19–36.

Urli M., Porté A.J., Cochard H., Guengant Y., Burlett R. & Delzon S. (2013) Xylem embolism threshold for catastrophic hydraulic failure in angiosperm trees. *Tree Physiology* **33**, 672–683.

Venturas M.D., Pratt R.B., Jacobsen A.L., Castro V., Fickle J.C. & Hacke U.G. (2019) Direct comparison of four methods to construct xylem vulnerability curves: Differences among techniques are linked to vessel network characteristics. *Plant, Cell & Environment* **42**, 2422–2436.

Wapstra M., Thompson I. & Buchanan A. (2008) An illustrated and annotated key to the Tasmanian species of *Senecio* (Asteraceae). *Kanunnah* **3**, 49–93.

Wilkening J. V., Skelton R.P., Feng X., Dawson T.E. & Thompson S.E. (2023) Exploring within-plant hydraulic trait variation: A test of the vulnerability segmentation hypothesis. *Plant, Cell & Environment*.

Wolfe B.T., Sperry J.S. & Kursar T.A. (2016) Does leaf shedding protect stems from cavitation during seasonal droughts? A test of the hydraulic fuse hypothesis. *New Phytologist* **212**, 1007–1018.

Zhang F.P. & Brodribb T.J. (2017) Are flowers vulnerable to xylem cavitation during drought? *Proceedings of the Royal Society B: Biological Sciences* **284**.

TABLES

Table 1. Water potentials (MPa) at 12, 50, and 88% cumulative embolism (P_{12}, P_{50}, and P_{88}) for leaf, upper stem, and basal stem of *Solanum lycopersicum* and *Senecio minimus*.

Species	Trait	Leaf	Upper stem	Basal stem
Solanum lycopersicum	P_{12}	-0.96 ± 0.12^{a}	-0.96 ± 0.11^{a}	-1.63 ± 0.17^{b}
	P_{50}	-1.21 ± 0.09^{a}	-1.43 ± 0.16^{a}	-2.31 ± 0.26^{b}
	P_{88}	-1.50 ± 0.09^{a}	-1.89 ± 0.20^{a}	-3.12 ± 0.29^{b}
Senecio minimus	P_{12}	-1.45 ± 0.06^{a}	-1.99 ± 0.12^{b}	-2.81 ± 0.11^{c}
	P_{50}	-1.92 ± 0.15^{a}	-2.28 ± 0.02^{a}	-3.22 ± 0.09^{b}
	P_{88}	-2.35 ± 0.05^{a}	-2.58 ± 0.02^{a}	-3.59 ± 0.11^{b}

Data are means ± SE (n = 5 for *Solanum* and n = 3 for *Senecio*). Different letters denote differences between plant tissues within the same species (Tukey's Test, $p < 0.05$).

Table 2. Time for the upper stem to reach critical water potentials (P_{12}, P_{50}, and P_{88}) relative to the basal stem region of *Solanum lycopersicum* and *Senecio minimus*.

Species	P_{12}	P_{50}	P_{88}
Solanum lycopersicum	0.51 ± 0.10*	0.59 ± 0.05*	0.63 ± 0.06*
Senecio minimus	0.54 ± 0.04*	0.54 ± 0.04*	0.56 ± 0.05*

Data are means ± SE (*n* = 5 for *Solanum* and *n* = 3 for *Senecio*). Asterisks denote differences between the upper stem and the stem base in their time to reach P_{12}, P_{50}, and P_{88} (Student's t-test, $p < 0.05$).

Table 3. Stem area (A_{stem}), xylem area (A_{xylem}), pith area (A_{pith}), xylem vessel diameter (D_h), the xylem cell wall thickness (t) and lumen breadth (b) ratio $(t/b)_3$, and the theoretical stem water flow rate (J_v) for the herbaceous upper stem and the woody basal stem regions of *Solanum lycopersicum* and *Senecio minimus*.

Trait	*Solanum lycopersicum*		*p*-value	*Senecio minimus*		*p*-value
	Upper stem	Basal stem		Upper stem	Basal stem	
A_{stem} (mm^2)	19.20 ± 1.18	71.14 ± 4.44	<0.01	18.07 ± 0.13	26.64 ± 1.38	<0.01
A_{xylem} (mm^2)	2.94 ± 0.20	31.29 ± 2.27	<0.01	4.16 ± 0.41	13.19 ± 0.87	<0.01
A_{pith} (mm^2)	10.67 ± 0.66	13.86 ± 1.97	0.16	10.56 ± 0.38	2.38 ± 0.47	<0.01
D_h (µm)	60.84 ± 3.77	76.41 ± 2.79	0.01	25.67 ± 0.62	29.51 ± 1.18	0.04
$(t/b)^3 \times 10^3$	2.73 ± 0.34	3.79 ± 1.15	0.40	9.93 ± 1.83	14.40 ± 2.08	0.42

Data are means ± SE (n = 5 for *Solanum* and n = 3 for *Senecio*). *p*-values < 0.05 denote statistical difference between upper and the basal portions of the stem according to Student's t-test.

FIGURES

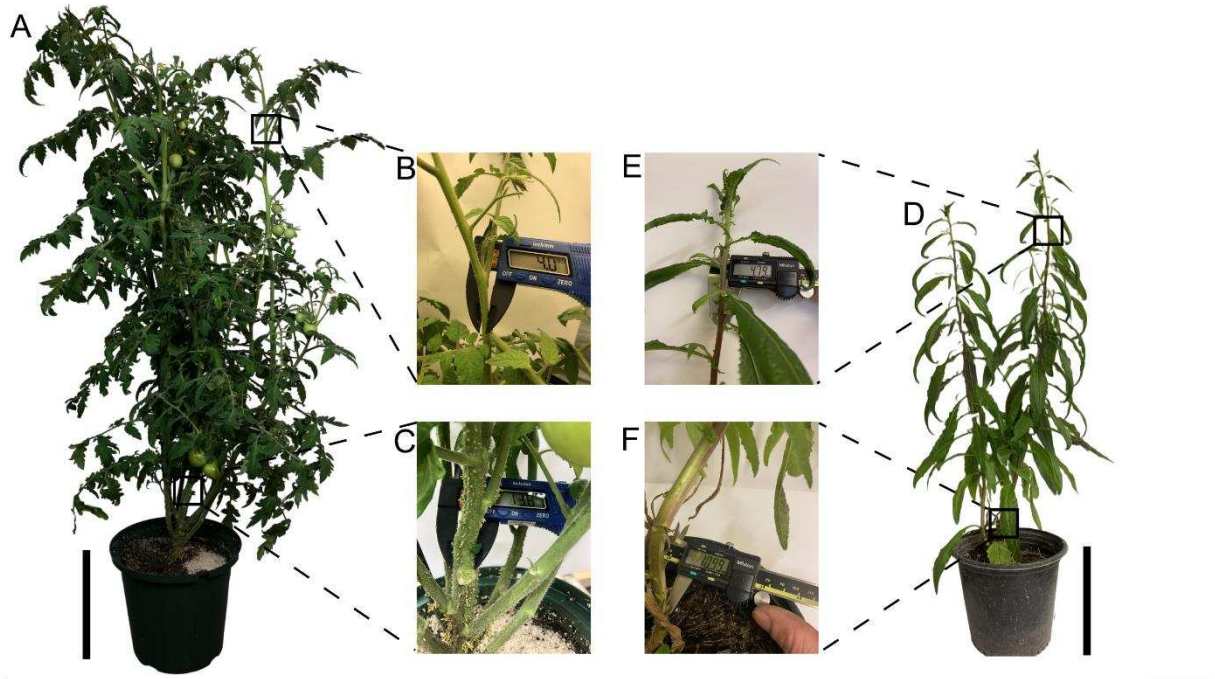

Figure 1. Plants of *Solanum lycopersicum* (five months old) (A) and *Senecio minimus* (seven months old) (D) and details of the upper stem (B, E) and the woody basal stem (C, F). Digital calipers (mm) are used to demonstrate differences in diameter between the upper and basal stems. Scales = 25 cm.

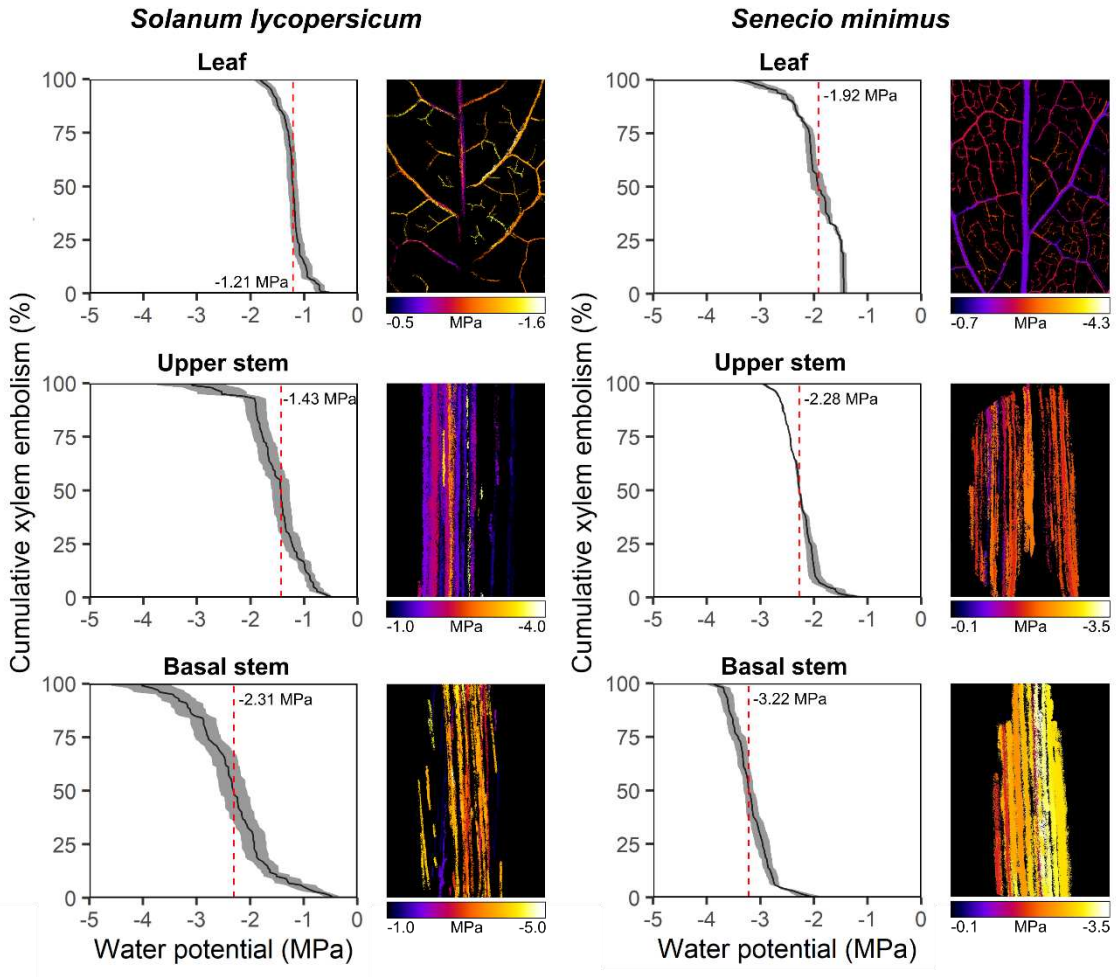

Figure 2. Optical vulnerability curves for leaf, upper and basal stem regions of *Solanum lycopersicum* and *Senecio minimus*. Solid black lines and shadows represent means ± SE (*n* = 5 for *Solanum* and *n* = 3 for *Senecio*). Red dashed lines indicate the water potential at 50% cumulative embolism (P_{50}). Color maps show the leaf water potentials at which the different embolisms occurred.

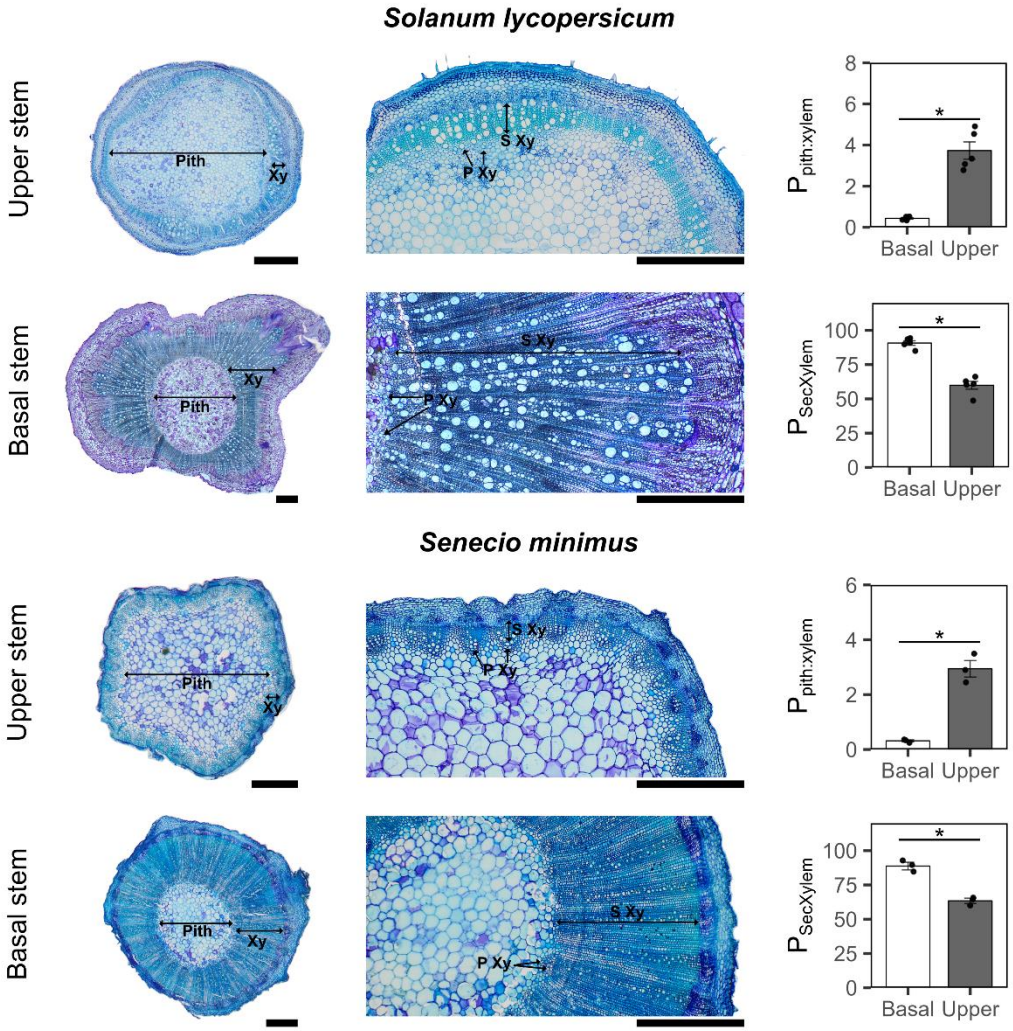

Figure 3. Cross sections of the upper stem and the basal stem of *Solanum lycopersicum* and *Senecio minimus* showing representative proportions of the pith and the xylem (Xy) as well as a detailed view of the primary (P Xy) and secondary xylem (S Xy). Pith-to-xylem area ratio ($P_{pith:xylem}$), proportion of secondary xylem vessel as a proportion to total xylem vessels ($P_{SecXylem}$) are shown for the herbaceous upper stem and the woody basal stem for both species. Bars are means ± SE (*n* = 5 for *Solanum* and *n* = 3 for *Senecio*) and black points are individual values. Asterisks denote statistical (*p-value* < 0.05) differences between the upper and the basal stems according to Student's t test. Scales = 1 mm.

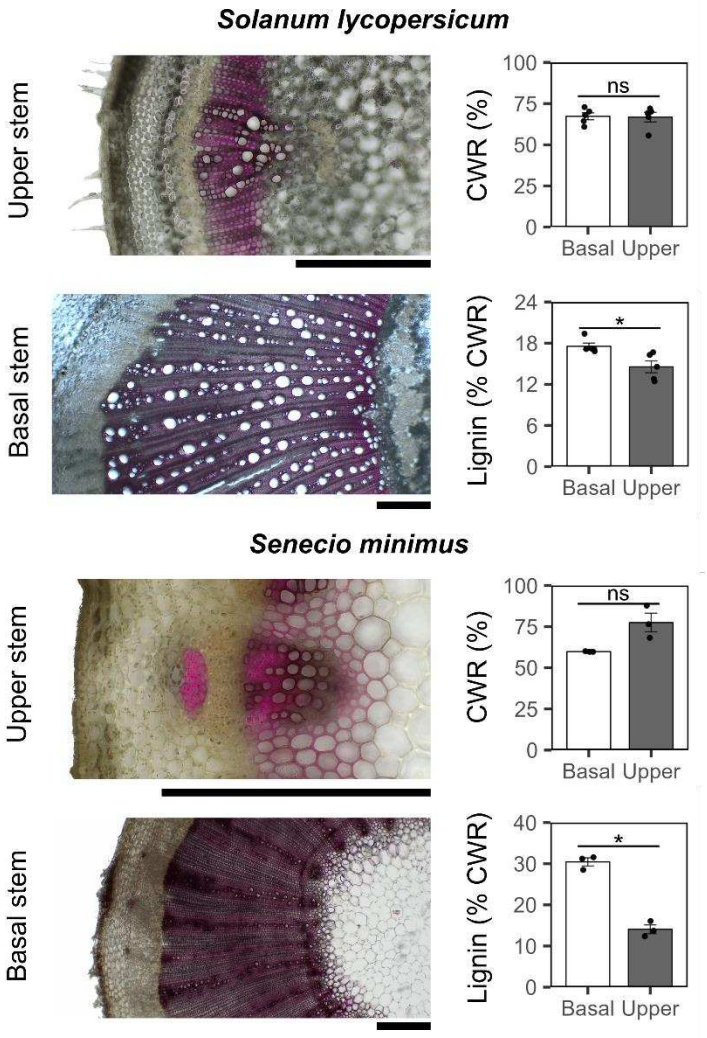

Figure 4. Lignin deposition at the upper and basal regions of the stems of *Solanum lycopersicum* and *Senecio minimus*. Patterns of deposition were assessed by staining the stem cross sections with phloroglucinol, which stains lignin in red. Differences in cell wall residue (CRW) (mg CWR mg dry weight^{-1} x 100) and lignin concentration (mg lignin mg CWR $^{-1}$ x 100). Bars are means ± SE (*n* = 5 for *Solanum* and *n* = 3 for *Senecio*) and black points are individual values. Asterisks denote statistical (*p-value* < 0.05) differences between the upper and the basal stems according to Student's t test. Scales = 500 µm.

SUPPLEMENTARY MATERIAL

Supplemental Table S1. Nutrient solution used for cultivation of *Solanum lycopersicum*.

Stock solution		Formula Weight	kg m^{-3} of stock solution
A	$Mg(NO_3)_2 .6H_2O$	256.41	26
	$Ca(NO_3)_2 .4H_2O$	236.15	64
	Sequestrene 330 Fe 10% Fe		10
B	KNO_3	101.11	40.44
	NH_4NO_3	80.04	16
	KH_2PO_4	136.09	4.8
	K_2HPO_4	174.18	5.6
	K_2SO_4	174.27	6
	Na_2SO_4	142.04	6.8
	H_3BO_3	61.83	0.28
	$MoO_3.2H_2O$	179.97	0.002
	$ZnSO_4.7H_2O$	287.54	0.011
	$MnCl_2.4H_2O$	197.9	0.0816
	$CuSO_4.5H_2O$	249.7	0.004
	$CoCl_2.6H_2O$	237.9	0.00024

GENERAL CONCLUSION

It was demonstrated that drought tolerance in young plants of tomato is highly dependent on the impact of ABA on stomatal function. Although there is a large variation in the constitutive ABA levels, the stem and leaves showed minimal differences in xylem embolism resistance. However, it was observed that genotypes with higher ABA levels, by altering the stomata density and size, exhibited lower maximum stomatal and minimum leaf conductance which efficiently improved water use efficiency under well-watered conditions and delayed hydraulic dysfunction. Furthermore, our findings indicate that older stems are more resistant to embolism due to increased woodiness as a consequence of the development of secondary growth. Structural and biochemical alterations underlying the higher embolism resistance in the woody base of stems include a lower pith-to-xylem area, a higher proportion of secondary xylem conduits, and higher lignin content. Such findings suggest that the improvements in the control of water loss resulting from increased ABA levels are likely more important than the increase in xylem resistance to embolism in young tomatoes, while the secondary growth can improve the drought resistance in later developmental stages, allowing the resprout under severe drought that might kill the upper canopy.